Technical Report Documentation Page

1. Report No.	2. Government Accession No.	3. Recipient's Catalog No.	
4. Title and Subtitle Evaluation of the Bettendorf Bridge, Iowa		**5. Report Date** **6. Performing Organization Code**	
7. Author(s)		**8. Performing Organization Report No.**	
9. Performing Organization Name and Address Center for Transportation Research and Education Iowa State University 2711 South Loop Drive, Suite 4700 Ames, IA 50010-8664		**10. Work Unit No. (TRAIS)** **11. Contract or Grant No.**	
12. Sponsoring Organization Name and Address		**13. Type of Report and Period Covered** **14. Sponsoring Agency Code**	
15. Supplementary Notes Visit www.ctre.iastate.edu for color PDF files of this and other research reports.			
16. Abstract			
17. Key Words		**18. Distribution Statement** No restrictions.	
19. Security Classification (of this report) Unclassified.	**20. Security Classification (of this page)** Unclassified.	**21. No. of Pages**	**22. Price** NA

Form DOT F 1700.7 (8-72) **Reproduction of completed page authorized**

EVALUATION OF THE BETTENDORF BRIDGE, IOWA

Final Report
July 2006

Principal Investigator
Terry J. Wipf
Director of the Bridge Engineering Center
Center for Transportation Research and Education, Iowa State University

Co-Principal Investigators
Brent M. Phares
Associate Director of the Bridge Engineering Center
Center for Transportation Research and Education, Iowa State University

F. Wayne Klaiber
Bridge Engineering Center Specialist
Professor of the Civil, Construction and Environmental Engineering Department
Center for Transportation Research and Education, Iowa State University

Research Assistant
Ursula Deza

Sponsored by
The Innovative Bridge Research and Construction
Federal Highway Administration

A report from
Center for Transportation Research and Education
IOWA STATE UNIVERSITY
2901 South Loop Drive, Suite 3100
Ames, IA 50010-8634
Phone: 515-294-8103
Fax: 515-294-0467
www.ctre.iastate.edu

TABLE OF CONTENTS

LIST OF FIGURES

LIST OF TABLES

ACKNOWLEDGEMENTS

The authors want to acknowledge to the Federal Highway Administration for providing the funding to complete this work. Also, they would like to thank the staff of the Bettendorf Public Works Department for all the assistance provided during this work.

EXECUTIVE SUMMARY

The objective of this study was to evaluate the structural performance of a bridge constructed with FRP deck panels that carries the 53rd Avenue extension over Crow Creek in Bettendorf, Iowa. To assess how the FRP panel deck behaves under actual bridge loading, field data were obtained from a long-term monitoring system and two short-term live load tests. This report summarizes the instrumentation, the test protocols, and the test results from this study. In addition and where applicable, the test results are compared with measured conventional-deck field behavior and empirical design assumptions.

The three-span bridge was constructed using funding provided through The Federal Highway Administration's (FHWA) Innovative Bridge Research and Construction (IBRC) program. Three different deck material combinations were used in the bridge deck. The west and middle span decks were continuously constructed with cast-in-place concrete reinforced with epoxy coated steel and glass Fiber Reinforced Polymer (GFRP) bars, respectively. The east bridge deck was simply constructed with pultruded FRP panels. The bridge is 173 ft – 7.5 in. long, 98 ft – 8 in. wide, and the deck system is supported by prestressed concrete (PC) girders.

The short-term testing consisted of monitoring the bridge behavior under controlled live loading. During these tests, strain data were obtained from twelve of the girders in the FRP-deck span and six of the girders in the reinforced concrete (RC) span. Additionally, strain data were also collected for the FRP panels themselves. During these tests, the bridge was loaded by driving a loaded tandem axle dump truck across the bridge at crawl speed. To investigate various aspects of the bridge performance, the test truck was driven in six transverse paths which were selected to either produce maximum response levels or represented typical traffic patterns.

By reviewing the recorded strains, it was determined that there were no significant changes in strain levels between the two tests which were separated by approximately one year. In fact, in some cases there were slightly lower readings in the second year. In general, based on the data collected, there was no significant loss of stiffness in the FRP-deck span during the two-year monitoring period.

The load distribution fractions (LDFs) were calculated using the measured bottom flange girder strains. As expected, the most critical loading condition occurred when the truck was driven close to the barrier. The resulting maximum LDF in the FRP-deck span was 47% in 2003, and 43% in 2004. For the same loading, the LDF in the RC deck span was 43% in 2003, and 41% in 2004. The neutral axis of the composite section was computed to evaluate the deck-to-girder connectivity. These calculi were based on the gage locations and field collected strain data. For comparison, theoretical calculations of the neutral axis location (provided by the designer), assuming full composite action, were also made. From the test results, it was observed that some of the girders may have achieved composite action and others may not have. The results also indicated that the central girders were resisting a notable level of torsional forces that were neglected in the original design. In general, it was also observed that the central girders may not have achieved full composite action with the FRP deck panels. Despite these findings, the measured strain levels were below the design values thereby giving assurance that the torsional effects and partial composite action may not be significantly impacting the strength of the prestressed girders.

The maximum differential horizontal displacement between the concrete girders and the FRP panel deck doubled from 2003 to 2004. The maximum slip in 2004 was 0.004501 in. When

tested in the laboratory, this level of slip occurred at a horizontal shear force of 19.5 kip, which is approximately 52% of the measured ultimate strength.

A walk-through inspection of the FRP deck, in 2004, revealed clear signs of cracking in the transverse direction. These cracks were found to be regular and are likely resulting from differential displacements between panels resulting from failed panel-to-panel connections.

1. INTRODUCTION

1.1. Background

Although Fiber Reinforced Polymer (FRP) composites have been extensively researched and used by other industries, FRP bridge deck panels have been designed and built without the benefit of nationally accepted standards. If FRP composite materials have a future in the bridge engineering industry, it must be determined how these complex materials react in actual bridge-loading environments. To this end, several bridges have been constructed nationwide with FRP composites like the Martin Marietta's DuraSpan® system deck. One of these bridges is the 53rd Avenue extension bridge over Crow Creek, located in Bettendorf, Iowa. This three-span bridge was constructed using funding provided through The Federal Highway Administration's (FHWA) Innovative Bridge Research and Construction (IBRC) program and is the subject of this report. It should be noted that the west and middle bridge decks were built with cast-in-place concrete reinforced with epoxy coated steel and glass Fiber Reinforced Polymer (GFRP) bars, respectively. The east bridge deck was built with the innovative FRP pultruded panels. Interestingly, this is the first FRP bridge deck in the United States to use composite action with prestressed concrete girders and at the time of construction was also the widest FRP deck (98 ft – 8 in).

1.2. Scope and Objective

The objective of this work was to evaluate the structural performance of the 53rd Avenue extension bridge constructed with FRP deck panels. For this purpose, two types of testing were utilized: short-term live load tests and long-term monitoring.

The scope of this work consisted of:

- The evaluation of test results from the two short-term live load tests with respect to:
  - The strain levels of FRP panels and the prestressed concrete (PC) girders.
  - The lateral load distribution fractions computed from field data and compared with the AASHTO Standards (1996) and AASHTO Specifications (1998).
  - The neutral axis locations for determining the level of the composite action.
  - The deck-to-girder slip to evaluate the shear connectors.
- The examination of the strain levels of the PC girder during the long-term monitoring.

1.3. Literature Review

FRP composite decks have been used in lieu of conventional construction materials on approximately 40 bridges nationwide (O'Connor, 2003). Noticeably, over half of these bridges

were built with DuraSpan® 766 deck. Herein, details of that deck system as well as tests on the deck are described.

1.3.1. DuraSpan® – Fiber-Reinforced Polymer Bridge Deck Systems (Martin Marietta Composites, 2005)

The DuraSpan® composite panel is comprised of individual pultruded tubes. The pultruded material is composed of E-glass fibers in various fiber orientations and an isophthalic polyester resin binder. The tubes are manufactured by Creative Pultrusions, Inc, and assembled into panels using adhesive by the Martin Marietta Company (Figure 1). Finishing of the panels consists of the cutting of the holes, sealing and installation of edge closeouts, and finishing of the surface. The length of the panels is typically set equal to the width of the bridge. Advantages of the FRP panels are that they resist corrosion and freeze-thaw cycles, are thought to outlive conventional materials, and have a high strength-to-weight ratio.

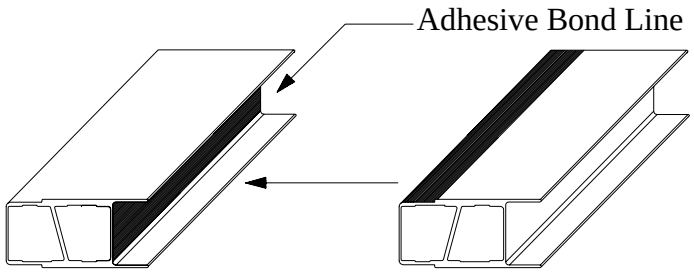

Figure 1. DuraSpan Deck Panel – Assembly Scheme

Two kinds of deck configurations are fabricated by Martin Marietta: one is 5 in. deep and weighs 13 lb per square foot and has an allowable beam spacing of 5 ft. The other configuration is 7.66 in. deep and weighs 19 lb per square foot with an allowable beam spacing of 10 ft. According to the manufacturer, the well-balanced and quasi-isotropic fabrics yield a highly durable deck. Additionally, this material can possess a high strength safety factor and has negligible fatigue and creep properties. The panels have the capability of achieving composite action with both prestressed concrete and steel girders.

1.3.2. Connection Tests of FRP Deck Specimens for Composite Construction – D. Wood, D., T.J. Wipf and F.W. Klaiber (June 2001)

Prior to the Duraspan® deck design and installation on the subject bridge, a standard push-out test, for the 53rd Avenue project only, was conducted in order to evaluate the proposed shear connectors. The objective of this testing was to determine the ultimate load capacity and the general load-deflection behavior. The detail was developed by the bridge owner and the bridge

design-fabricator team. In all three specimens were constructed and tested. The specimens consisted of a non reinforced concrete block with a strength of 7,000 psi. A haunch between the girder (i.e., the concrete block) and deck was simulated by ½-in. plywood. The FRP deck panels with slotted holes were placed over reinforcing bar hooks and grouted within the deck. With the FRP decks vertically positioned, specimens were loaded through the concrete block as shown in Figure 2.

The differential load-slip results showed very similar ultimate capacities; the average load was 78,387 (39,194 lb per connector). At the ultimate capacity, the maximum observed slip was 0.1 in. for Specimen 2 and 0.05 in. for Specimens 1 and 3. The failure mode observed could be described as concrete tension in all specimens along with an apparent bending of the steel connector in Specimen 2. The average initial stiffness, based on the load-slip results in the linear range, was 8,666 kip/in. (4,333 kip/in. per connector). Table 1 summarizes the ultimate applied load and the associated initial stiffness and the failure mode of three specimens. It should be noted that push-out tests likely represented the lower bound ultimate strength capacities for the hook shear connector detail because the non-reinforced concrete showed premature cracking. In general, the results provided useful behavioral information about the hook shear connectors after which the details were only slightly modified for the subject bridge.

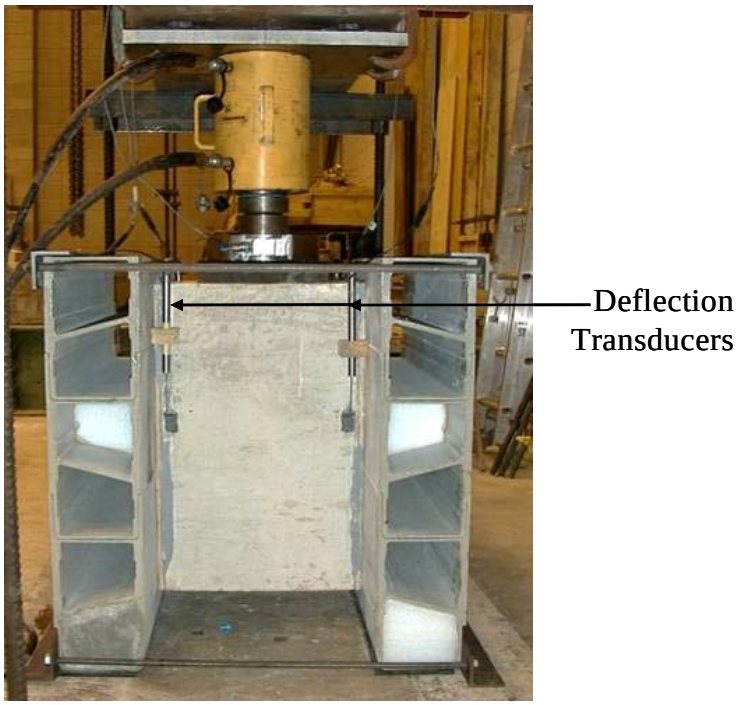

Figure 2. Typical Test Setup

Table 1. Summary of Laboratory Test Results of Three Specimens

Specimen	*Ultimate Applied* Load (lbs)*	*Initial Stiffness** (103 kips/in)*	*Failure Mode*
1	82,860	7.05	Concrete tension
2	75,880	9.69	Concrete tension and apparent steel bending
3	76,430	9.25	Concrete tension
Average	78,390	8.66	

Note: ** Total applied load; divide by two for the load on each shear connection.*
*** Based on load-slip deflection in linear range during Stage 3.*

1.3.3. Load Test and Rating Report Fairground Road Bridge, Greene County, Ohio – Bridge Diagnostic, Inc (November 2002)

The objective of this testing was to verify that a new FRP deck was acting compositely with the beams, to determine the lateral load transfer characteristics of the bridge, and to confirm that the refurbished bridge had higher load ratings than were indicated by traditional rating methods. The bridge is comprised of three spans – 68 ft, 85 ft, and 68 ft long. The superstructure consisted of four steel girders spaced at 9 ft – 4 in. and a 7.5-in. deep hollow core FRP deck with a 2-in. asphalt wearing surface. The orientation of the panels was in the transverse direction.

The instrumentation used in the Green County testing included 36 re-usable strain transducers and 4 Linearly Variable Displacement Transducers (LVDT). Strain transducers were installed on the four girders in two spans – both near the abutment and pier and at mid span. LVDTs were placed above the pier to measure deflections in the FRP deck. Additional strain transducers were placed on the underside of the deck to check for composite behavior and transverse strain magnitudes. A 69-kip dump truck crossed the bridge along pre-determined paths at a crawl speed. Each test was repeated twice in order to check reproducibility. One additional test was run at 45 mph.

The field data on the same path were examined graphically. The observed similarities demonstrated the elastic behavior of the structure. The collected data were used to aid in the development of a finite element model. The neutral axis locations on the beam were assessed and the composite action of the beam interacting with the FRP deck was verified for each girder. Only one beam showed a “low” neutral axis. This result was associated to a low bottom flange strain at the instrumented location and an observed loss of stiffness in the girder. The report underlined the possibility of localized variations in the strain that could be related to the gage position, the shear studs and grout pockets. From the gages placed longitudinally underneath the deck, the strain histories were determined to be similar to the steel beam response, verifying the

composite action between the deck and the beams at the instrumented locations. Based on the high-speed test, the impact factor was estimated to be 10%.

1.3.4. Fiber-Reinforced Polymer Bridge Decks, Status Report and Future – T. Keller, Bridge Design and Engineering (2004)

Currently, FRP composites are emerging as a promising alternative for bridge decks. The high strength combined with small dead load, large tolerance for freeze-thaw and de-icing salts, short installation times, and simpler construction details are some of the favorable advantages of the FRP materials over the conventional materials. A variety of different FRP deck systems have been developed and installed for demonstration projects. These demonstrations have been primarily on bridges with spans up to 30 ft. Multi-cellular deck panels made from adhesively bonded pultruded shaped tubes, and sandwich panels with different core configurations are the most commonly used.

Despite the positive characteristics of FRP bridge decks, the mechanical deck-to-girder connections are a point of concern. The load-carrying behavior of the sandwich deck is normally bi-directional while the behavior of the pultruded decks is unidirectional (in the direction of the pultrusion). Span limitations are also governed by serviceability. With regard to the fatigue resistance, sandwich decks seem to be more sensitive to fatigue loading. Part of this may be the result of poor quality control during the fabrication process. In contrast, FRP pultruded decks can resist 10 million cycles without any signs of damage or stiffness loss.

In order to expand the market for FRP bridge decks, some improvements must be made for both panel types. From this report, the increment of the deck thickness and new multi-cellular cross sections for FRP pultruded panels were recommended. For all deck types, it was recommended that the stiffness in the longitudinal direction be increased. Additionally, the fabrication process and new materials must be developed to decrease costs. The use of thermoplastic resins was suggested as a way of reducing both material and fabrication costs.

1.3.5. Thermal Response of Fiber Reinforced Polymer Composite Bridge Decks – H. GangaRao (CFC News, 2004)

The Constructed Facilities Center at the West Virginia University has extensively studied the thermal response of FRP pultruded decks. It was found that the temperature difference between the top and bottom surfaces can be as high as 120^{o}F, three times larger than found in concrete decks. The large temperature differences were attributed to the fact that the hollow portions of FRP deck were not able to distribute heat from the top surface to the bottom surface as effectively as solid concrete decks. Additionally, it is widely known that FRP composite materials have relatively low thermal conductivity.

A study conducted by GangaRao consisted of thermal tests on two kinds of FRP bridge decks (4-in. and 8-in. deep modules). In the laboratory, heating and cooling tests were carried out with different boundary conditions. During the heating test, the top surface was heated to around 150

to 155^{o}F using a propane heater. The bottom surface was kept at room temperature. In the case of the cooling test, the top surface was covered with dry ice, while the bottom was kept at room temperature. The top surface was cooled to around -20 to -40^{o}F, depending on the amount of dry ice. After the deck was returned to ambient temperature from cooling, no significant residual strains were observed. However, at the end of the heating cycle, residual strains ranging from 25 to 100 $\mu\varepsilon$ remained in the system.

In the field, thermal responses of two FRP bridges revealed that the compressive stresses were induced by direct exposure to the sunlight. For a temperature change of 100^{o}F at the deck top and 30^{o}F at the deck bottom, the induced thermal stresses could be at 45% of the allowable FRP deck stresses, and the induced thermal strain could be as high as 86% of the allowable FRP deck strains.

In conclusion, the repeated thermal cycles and high temperature differences through the depth of the FRP deck could cause high cumulative strains. This could be one of the reasons for commonly observed cracking in the wearing surface – especially at the field joints. The study recommended filling the cores with light foam that could more effectively transfer heat from the top to the bottom surface of the FRP deck. Another alternative proposed was the use of a bright color-wearing surface that could reduce the top surface temperature of the FRP deck under the sunlight exposure.

1.4. Report Summary

This final report is divided into six chapters. Chapter 1 presents the introduction, scope and objective, and a very brief literature review related to the application of FRP in bridges. The description of the subject bridge is given in Chapter 2. Chapter 3 presents the evaluation program and Chapter 4 summarizes the associated monitoring results. Chapter 5 summarizes the observations and conclusions.

2. BRIDGE DESCRIPTION

This subject bridge is the 53rd Avenue extension bridge designed by The Schemmer Associates (Omaha, Nebraska). The design of the FRP panels was completed by Martin Marietta. The Schemmer Associates verified this design and checked the prestressed girder stresses. The bridge is located over the Crow Creek in Bettendorf, seven miles from Davenport, in Scott County (Figure 3). It has three spans with no skew. Three different technologies were used for the bridge deck. The west and middle bridge deck sections were built continuously with cast-in-place reinforced concrete (RC); the west deck was reinforced completely with epoxy coated steel and the other with a combination of epoxy coated steel and glass Fiber Reinforced Polymer (GFRP) bars. The east deck was built independently with the previously described Martin Marietta pultruded deck panels. Figure 4 shows the plan view of the bridge.

The bridge is 170 ft – 7 in. long. The steel RC and GFRP-RC spans are 61 ft – 6 in. and 62 ft – 4 in. long, respectively. The FRP-deck span is 46 ft – 9 in. long (Figure 4). A typical cross section of the bridge comprises the roadway, a concrete median, and two sidewalks. Each deck system is supported by fourteen standard Iowa DOT prestressed concrete (PC) girders. At both edges, the deck supports two concrete barriers and two pedestrian handrails. The roadway carries three west-bound and two east-bound lanes of traffic. The deck has a crown of 2% that is coincident with the FRP panel joint underneath the concrete median (Figure 5).

Figure 3. Bettendorf Bridge – Looking East

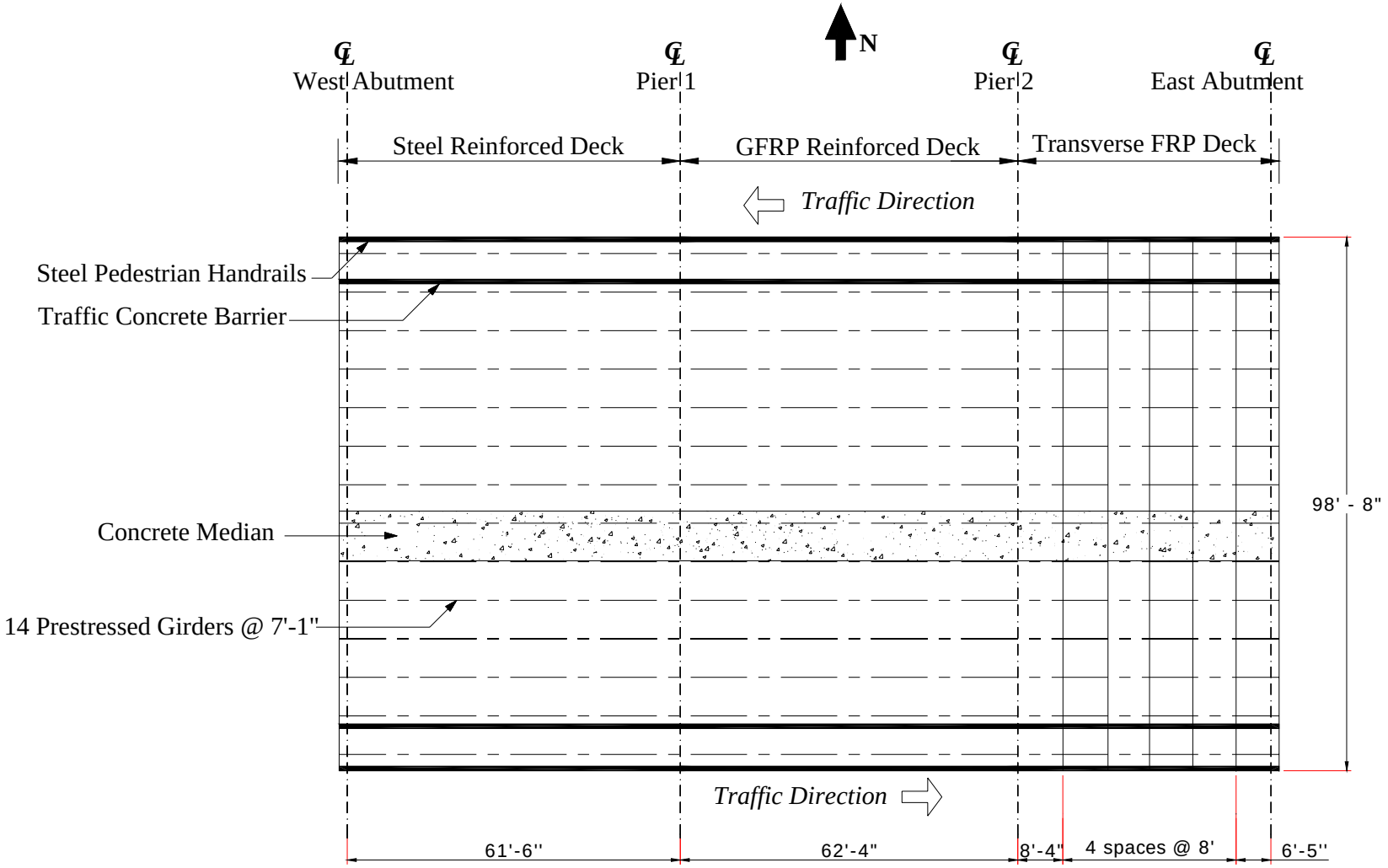

Figure 4. Plan View of the 53rd Avenue Extension Bridge

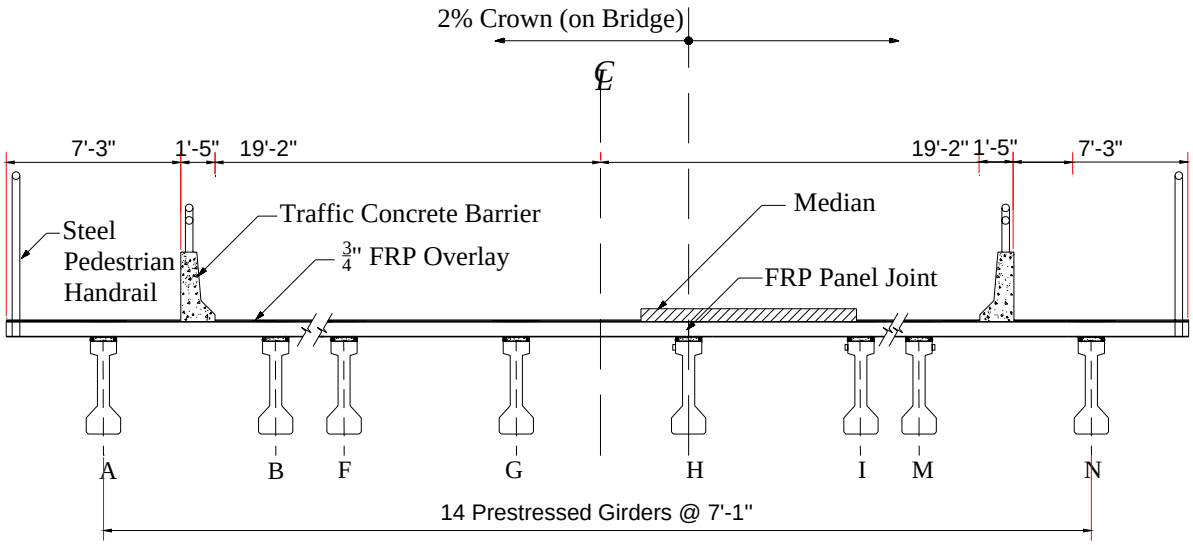

Figure 5. East View of FRP Panel Deck Cross Section

The longitudinal cross section and the lateral view of the FRP deck span are shown in Figure 6 and Figure 7, respectively. The PC girders are interconnected with bolted intermediate diaphragms. It should be noted that the bridge has an integral abutment on the east bridge end. Over Pier 2, the PC beams were separated by 2 in. to support the steel and GFRP RC deck and the FRP panel deck respectively, and to enclose the PC girder ends. A 2-in. preformed compression seal was used to form the expansion joint between the two decks.

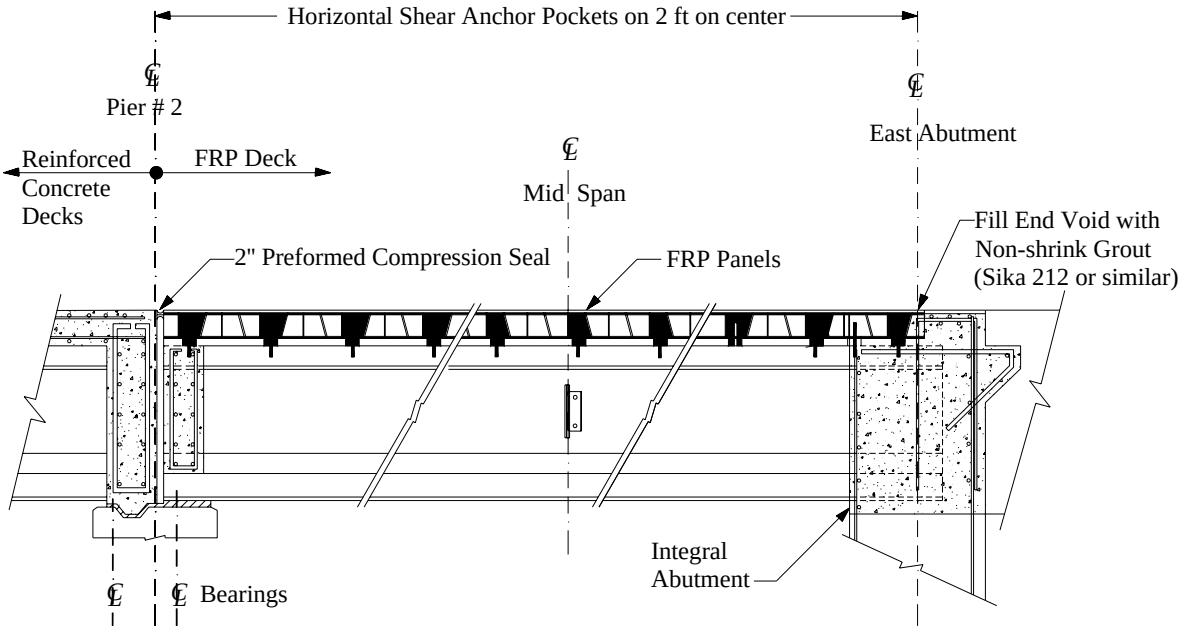

Figure 6. Longitudinal Cross Section of the FRP Deck Span

Figure 7. Expansion Join Detail

For the FRP deck span, a total of twelve DuraSpan® 766 panels (thickness equivalent to 7.66 in.) manufactured by Martin Marietta (9) were installed. The panels were fabricated with the dimensions shown in Figure 8. Also, the pre-drilled top and bottom holes, spaced at 24 in., were factory installed (Figure 9).

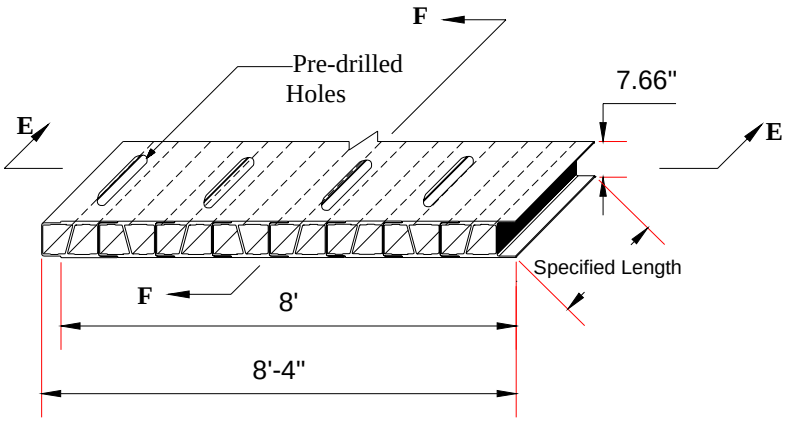

Figure 8. Typical FRP Deck Panel

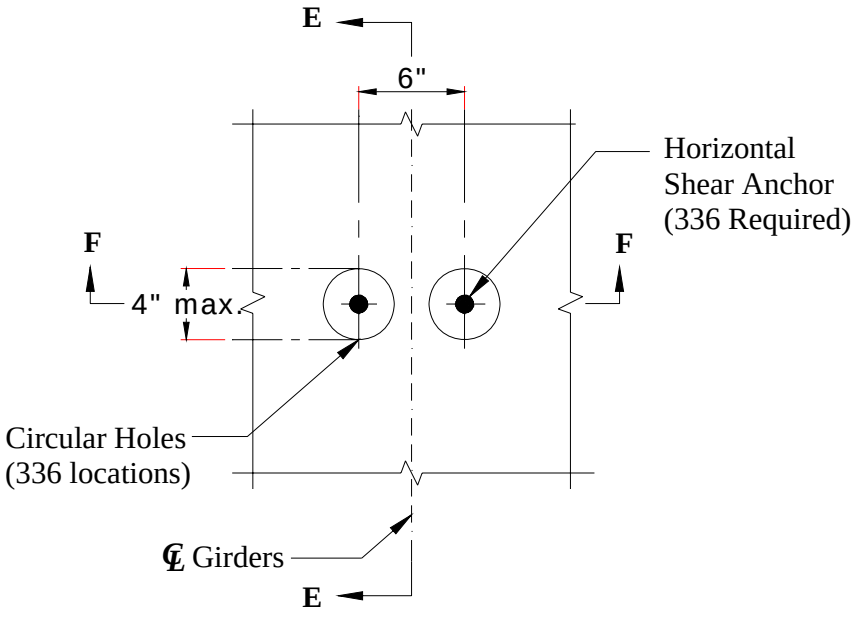

Figure 9. Bottom View of the Holes in Deck Panels

Two 4-in. deep holes were pre-drilled every 24 in. on the top flange of the PC girders to hold 3/4-in. u-shape shear stirrups fixed with a two-part epoxy. Between the panels and the girders, two polystyrene supports were attached with adhesive to form the haunch (varying from approximately 1 in. to 2 in. thick) (Figure 10). The panels were interconnected by three 6-in. wide FRP splices on the top. The FRP deck holes were filled with non-shrink grout to create composite action as was previously described. Figure 11 shows the connection detail between the PC girders and FRP panels. Figure 12 shows the top deck prior to the placement of the wearing surface, while in Figure 13, the bottom of the deck and the intermediate diaphragms are shown. Finally, Figure 14 shows the 3/4-in. two-part polymer concrete (epoxy and rock chips) wearing surface that sealed and leveled the adjacent surface with concrete deck and approach pavement.

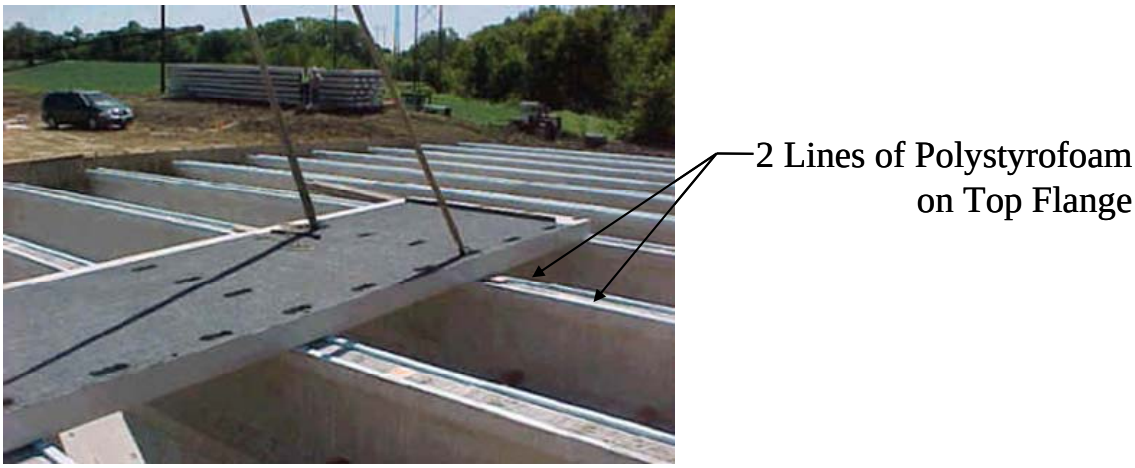

Figure 10. Installation of the FRP Panel Deck

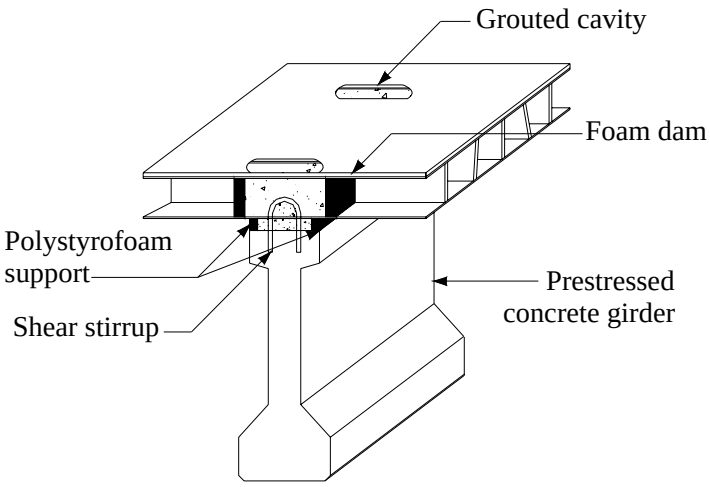

Figure 11. Composite Action: FRP Panel and Prestressed Concrete Girder

Figure 12. FRP Deck - Top Surface

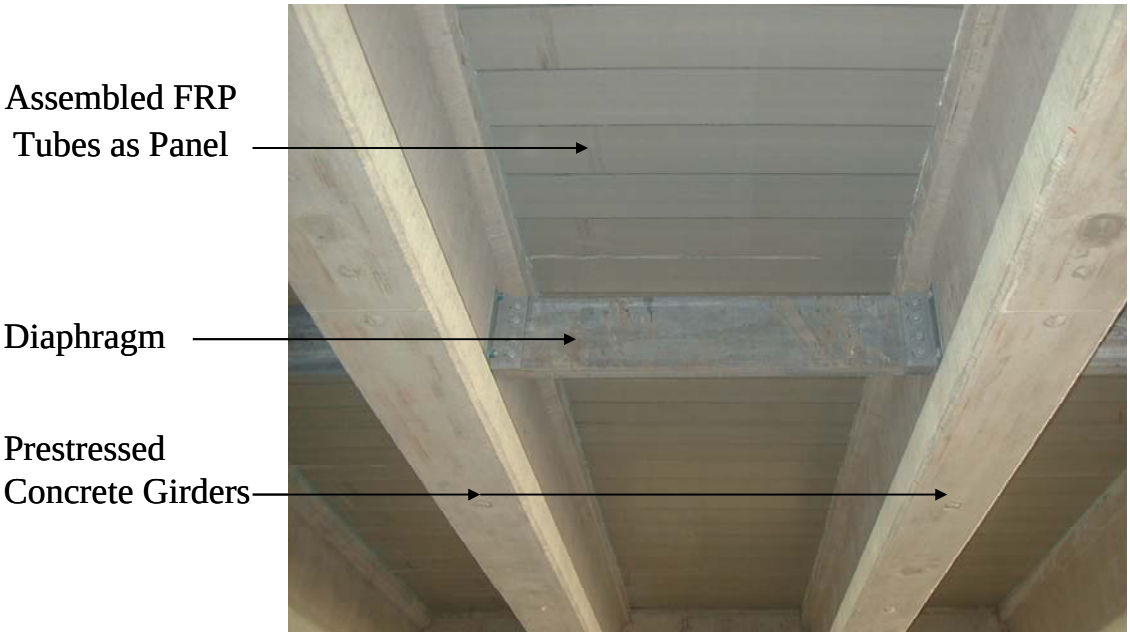

Figure 13. FRP Deck - Bottom Surface

Figure 14. FRP Deck – May 2003

To attach the concrete barrier rail to the FRP deck, stirrups were anchored in the deck with non-shrink grout. It should be noted that the barrier railing on the FRP deck span was constructed separately from the rest of the rail system to ensure thermal compatibility. The bridge was opened to traffic in May 2003.

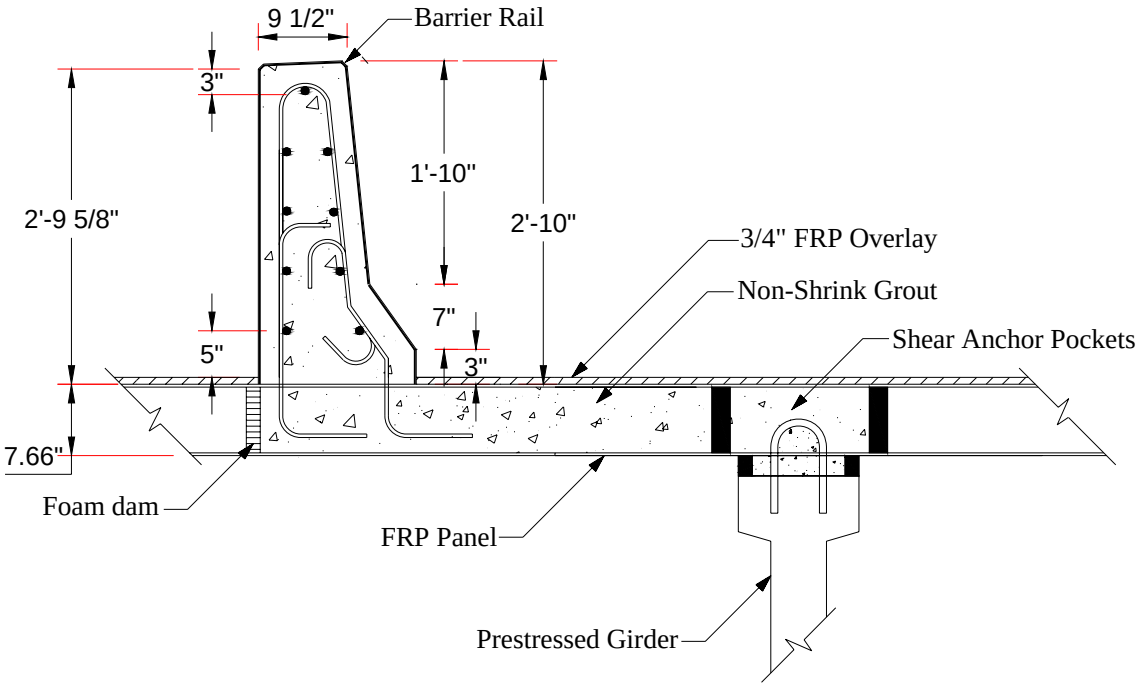

Figure 15. Barrier Cross Section

3. FIELD EVALUATION PROGRAM

Field monitoring was performed on the subject bridge to assess the performance of the new material. Instrumentation was placed at important locations to collect displacement and strain data. The testing program consisted of two short-term tests and long-term monitoring of the bridge. In the following sections, both monitoring programs are described.

3.1. Short – Term Monitoring

Live load tests on the 53rd Avenue Bridge were conducted on May 22, 2003 and May 13, 2004. The test protocol consisted of monitoring the behavior of the bridge under controlled loading. Instrumentation used for this testing was designed to measure attributes of significance in assessing the overall performance of this type of structure. Specifically, strains in the FRP deck and PC girders of two spans (the FRP deck span and the conventionally RC deck span) were measured. In addition, horizontal slip between the FRP deck and several bridge girders was also measured. Figure 16 and Figure 17 illustrate the locations of the strain and slip instrumentations. Girder strains were measured in Girders B through M in the FRP deck span and Girders B through G in the conventional RC deck near the top and bottom flanges in all cases (Figure 18). Transverse strains in the FRP deck were measured in one panel at four locations to determine the general behavior of a typical deck panel. Horizontal slip, the relative displacement between the deck and girder, was measured at four locations to study the level of composite action present in the bridge. Figure 19 is a photograph of typical instrumentation used during the testing.

During all live load tests, the bridge deck was loaded by driving a loaded tandem axle dump truck (Figure 20) across the bridge at a crawl speed. To investigate various aspects of bridge performance, the test truck was placed in the six transverse positions illustrated in Figure 21. These positions, hereafter designated as Path Y1 through Path Y6, were selected because they either produced maximum response in certain members or represented typical traffic patterns. The 2003 truck weight was equal to 67,640 lb with 17,640 lb and 50,000 lb for the tandem axles, respectively (See Figure 23).

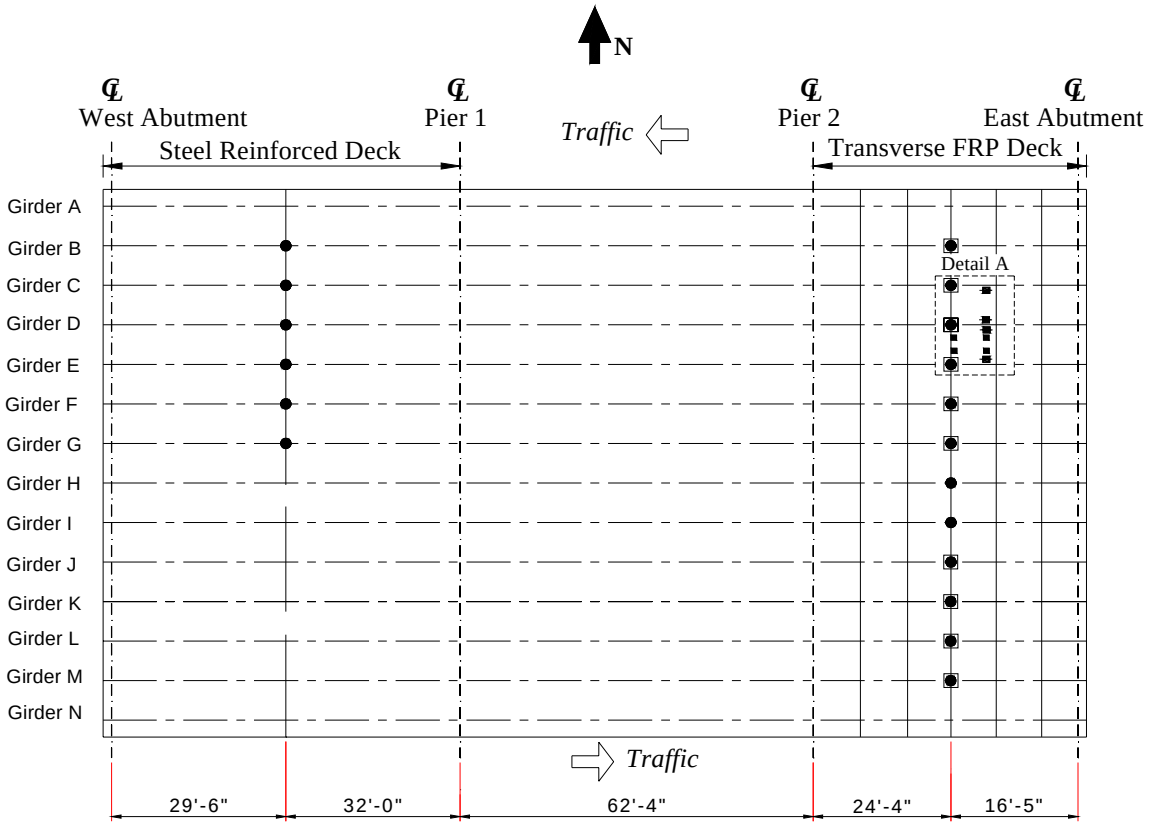

Note: • *Represent the strain transducers on the top and bottom flanges for the short-term live load test.*

 Represent the strain transducers on the bottom flanges for the long-term monitoring.

Figure 16. Overall Instrumentation Location

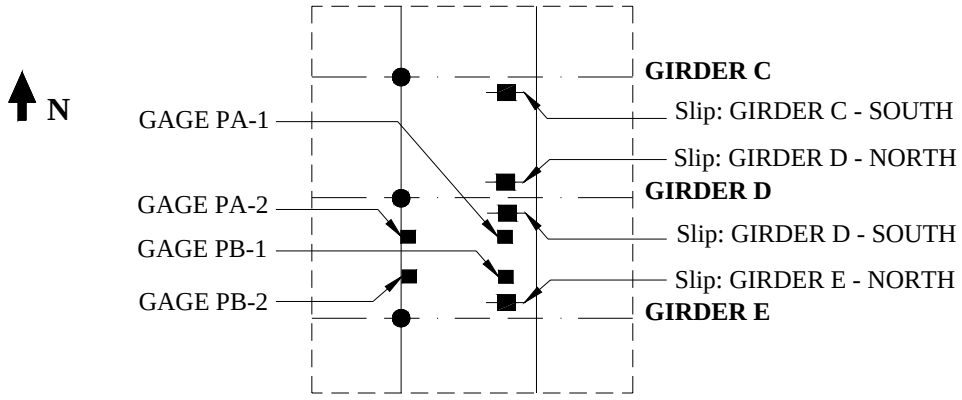

Figure 17. Instrumentation Details: Detail A

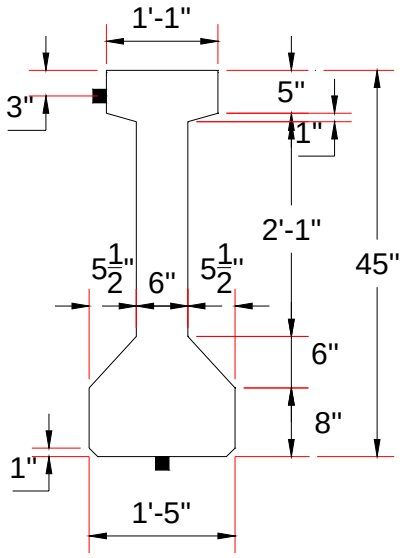

Note: ■ Strain Gage

Figure 18. Girder Strain Gage Placement

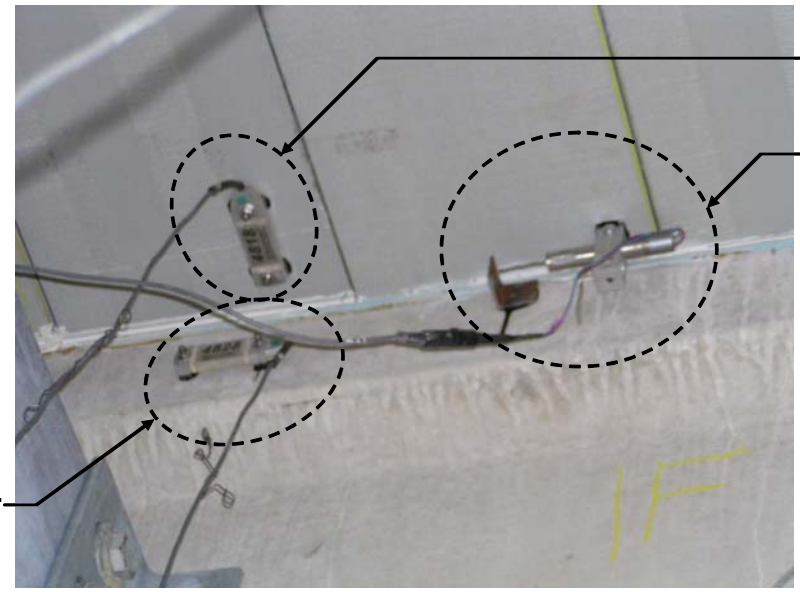

Figure 19. Photograph of Typical Transducers.

Figure 20. Test Load Truck.

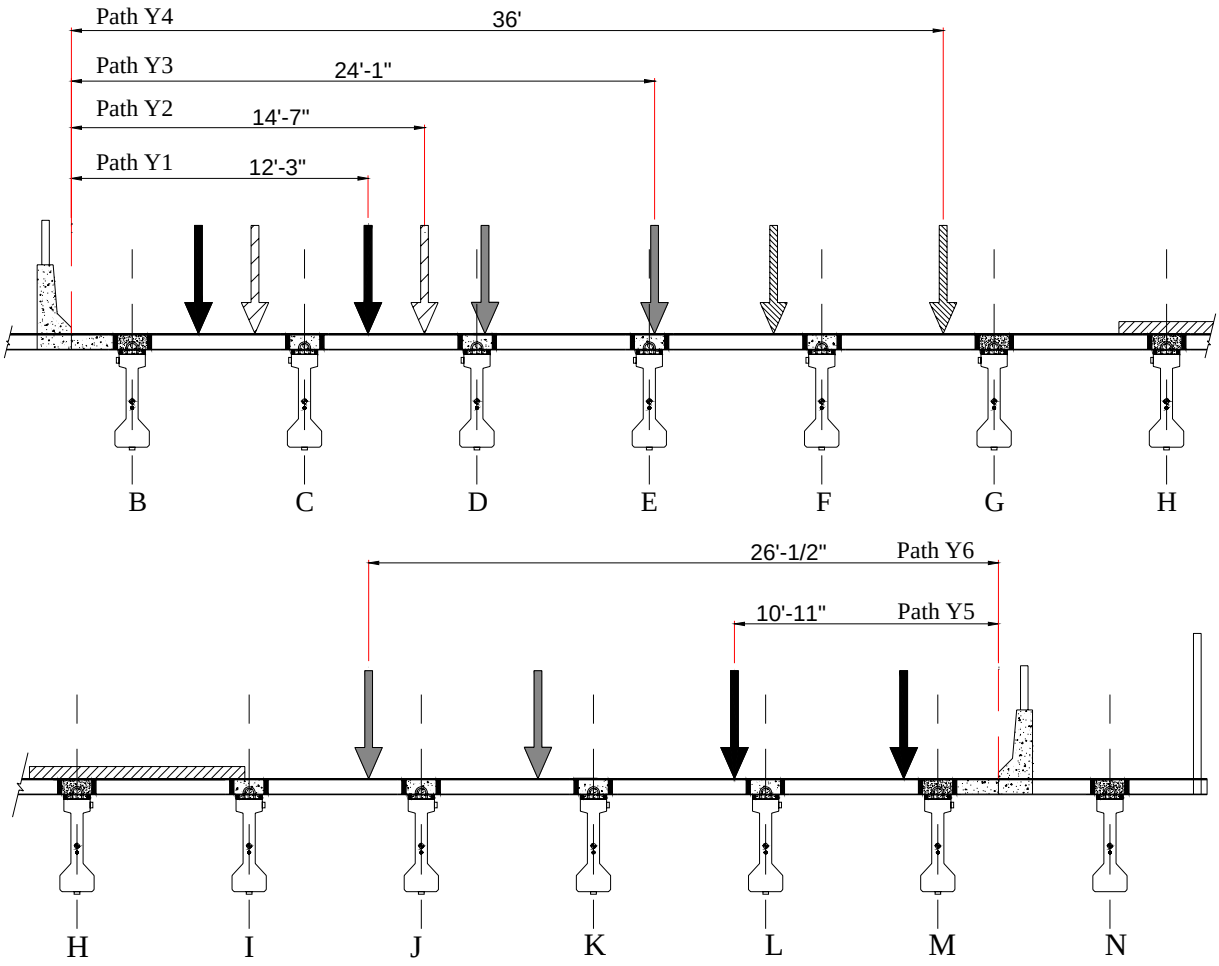

Figure 21. 2003 Test Paths: East View

The test performed in 2004 followed the same general protocol used in 2003. However, Paths Y3 and Y4 were offset approximately seven feet from the original paths. Figure 22 shows the 2004 truck paths. The truck used in both tests was the same; however, the 2004 truck weight was 65,960 lb, 2.4% below the 2003 weight. The front and rear-tandem axle weights were 17,040 lb and 48,920 lb, respectively (Figure 23).

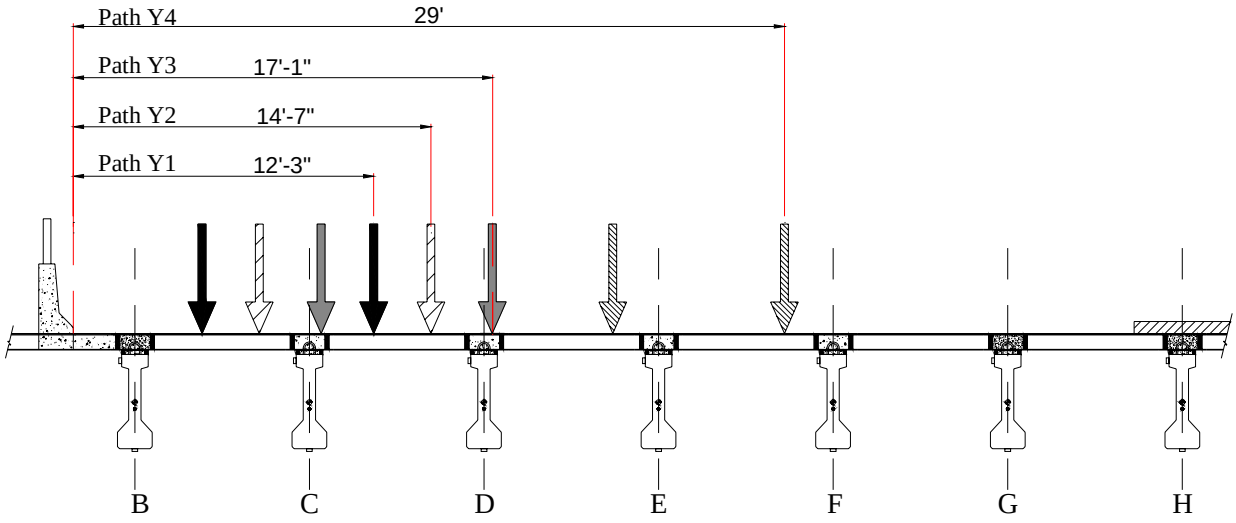

Figure 22. 2004 Test: Path Y3 and Y4 Modified

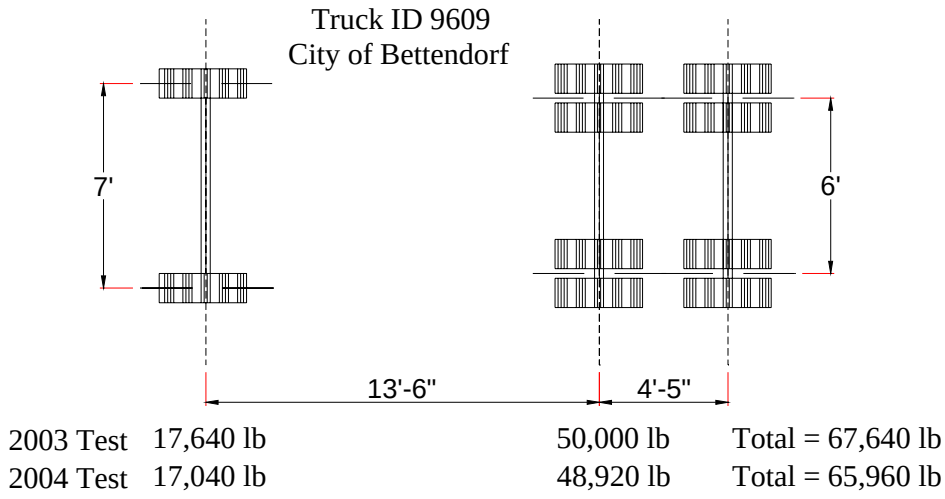

Figure 23. Geometry and Weight of Test Truck

3.2. Long – Term Monitoring

On September 26, 2003 a long-term monitoring system was installed on the 53rd Avenue Bridge. The long-term monitoring system was designed for the specific purpose of identifying if any unusually "large" loads crossed the bridge. Information on the passage of large loads was desired to allow an increased level of confidence that any observed deterioration was not the result of abnormal loadings and, therefore, could be attributed to bridge-specific parameters with a specific interest in the impact on the FRP bridge components.

The long-term monitoring system consisted of a passive strain sensor manufactured by Lifespan Technologies. These passive sensors continuously monitor and record the peak strain since installation. Ten peak strain sensors were installed at mid span of Girders B through G and Girders J through M as shown in Figure 16 (note that the peak strain sensors were located at the same position as the short-term live load test sensors). The ten sensors were installed on the girder shown during short-term testing to have the highest strain levels under ambient traffic. As with the short-term instrumentation, the peak strain sensors were installed at mid span of the span with the FRP deck panels. Photographs of sensors are shown in Figure 24 and Figure 25.

The passive peak strain sensors were monitored by connecting a data collection unit to each sensor one at a time. The data were collected approximately once every two weeks for just over two years.

In addition to the peak strain readings, the Lifespan Technologies sensors have the capability to report the current state of strain. Beginning on December 4, 2003 these data and an estimate of the ambient air temperature were also collected. The three types of data (peak strain, current strain, and ambient air temperature) were all used to assess the potential for the passage of an unusually large load.

Figure 24. Overall View of the Long-Term Monitoring System (Peak Strain Sensors)

Figure 25. Close Up View of an Installed Peak Strain Sensor

4. RESULTS

4.1. Short Term Monitoring Results

This section presents and compares the collected short-term test data. Strains and displacements presented here are referenced to the load truck position along the bridge, measured in feet. For convenience, truck position zero corresponds to the point of where the front tire of the truck crossed the bridge joint.

4.1.1. FRP Deck Strains

Figure 26 shows the truck loadings and the gage positions used on the bottom of the FRP panel deck and orientated in the direction of the panels. It should be noted that when the load was in the immediate vicinity of the gages, large and localized strain levels were observed. Based on the strain data collected on the FRP panel deck, in general, no significant changes in strain levels occurred between 2003 and 2004. In fact, as illustrated in Figure 27 and Figure 28 when the load was in Path Y2, the strains obtained during the 2004 Test were often lower than during the 2003 Test. During the 2003 Test, the largest recorded strain was 405 microstrains (MII) (Figure 29). During the 2004 Test, the maximum recorded strain was 231 MII (Figure 30).

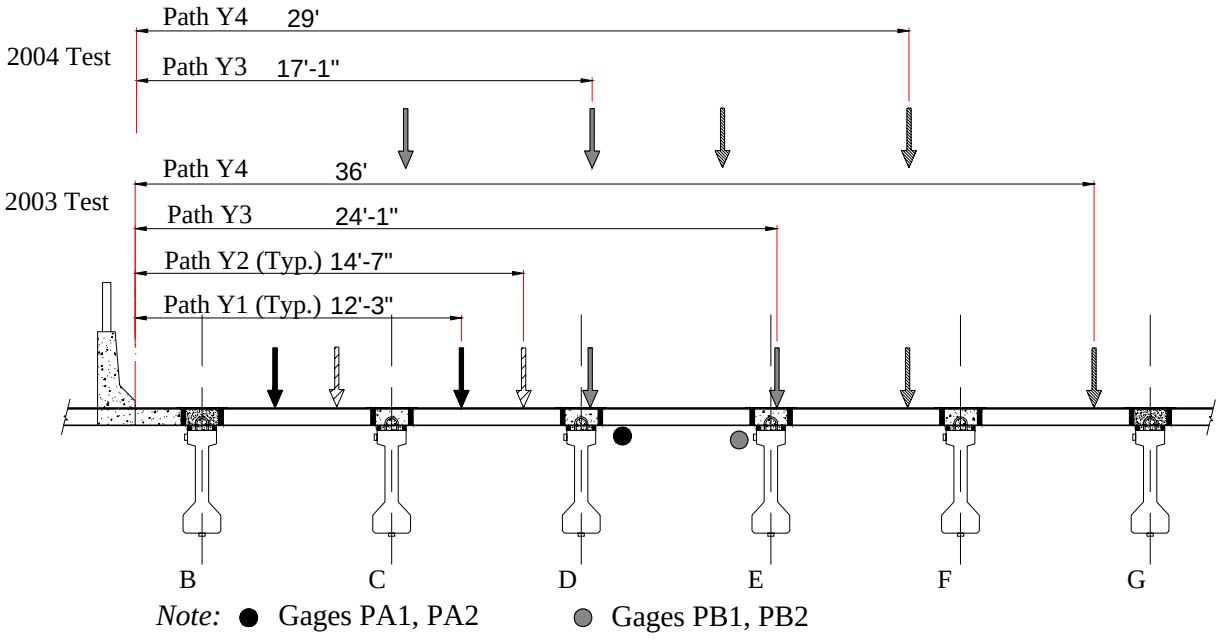

Figure 26. Gage Positions With Respect to Truck-Loading Path

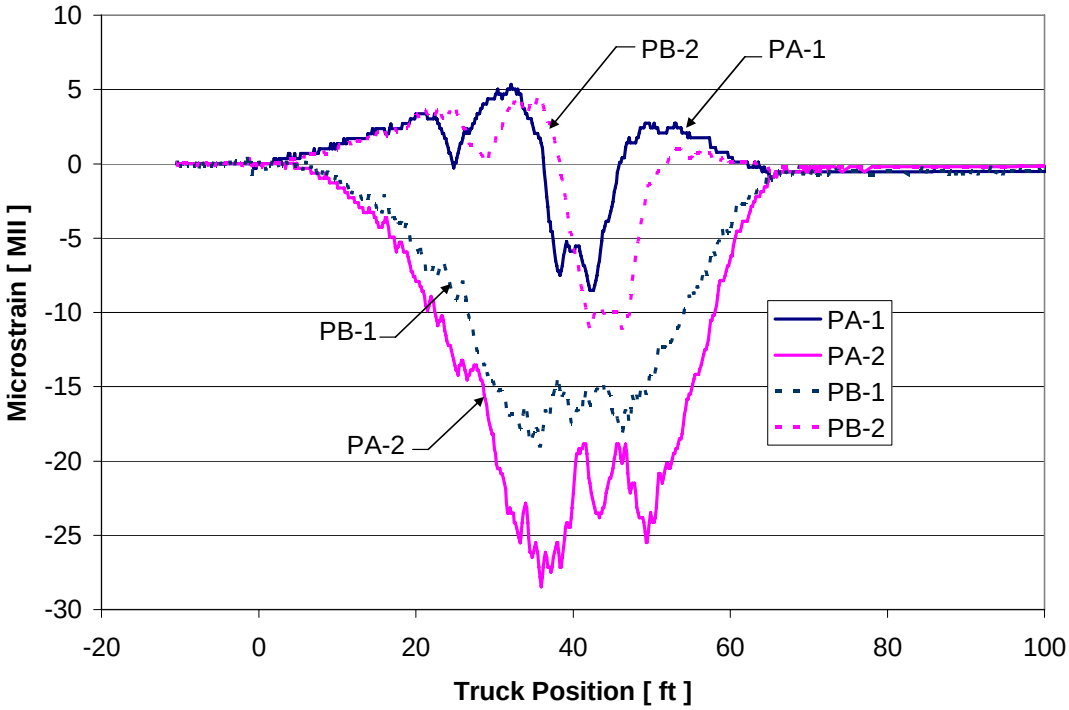

Figure 27. FRP Deck Strains: Path Y2 – 2003 Test

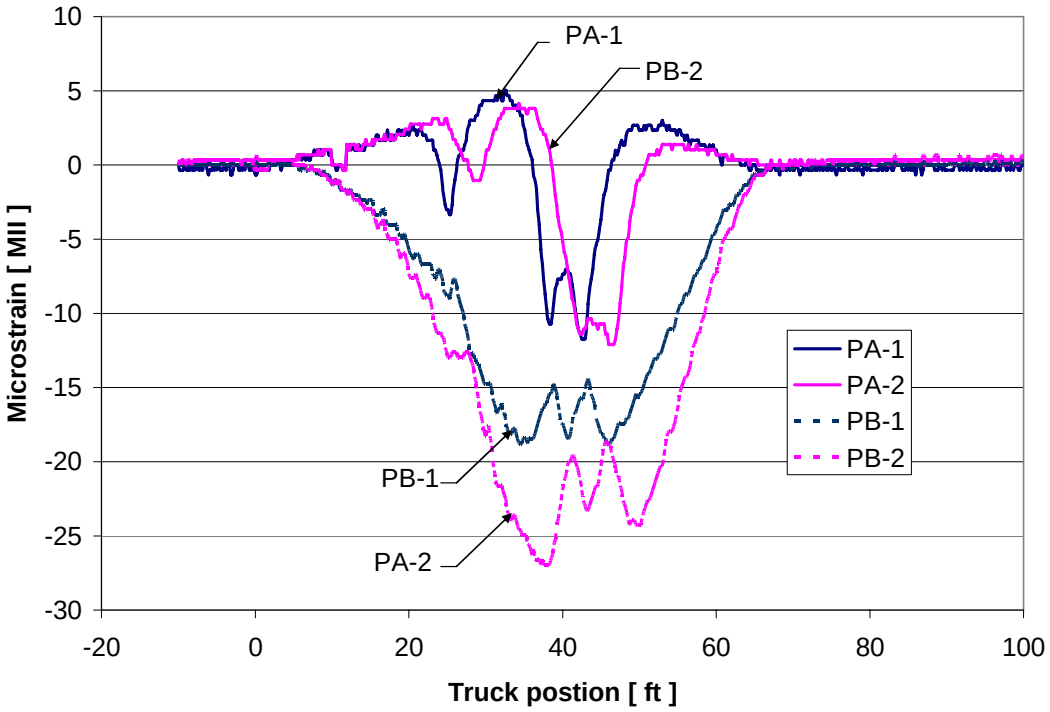

Figure 28. FRP Deck Strains: Path Y2 – 2004 Test

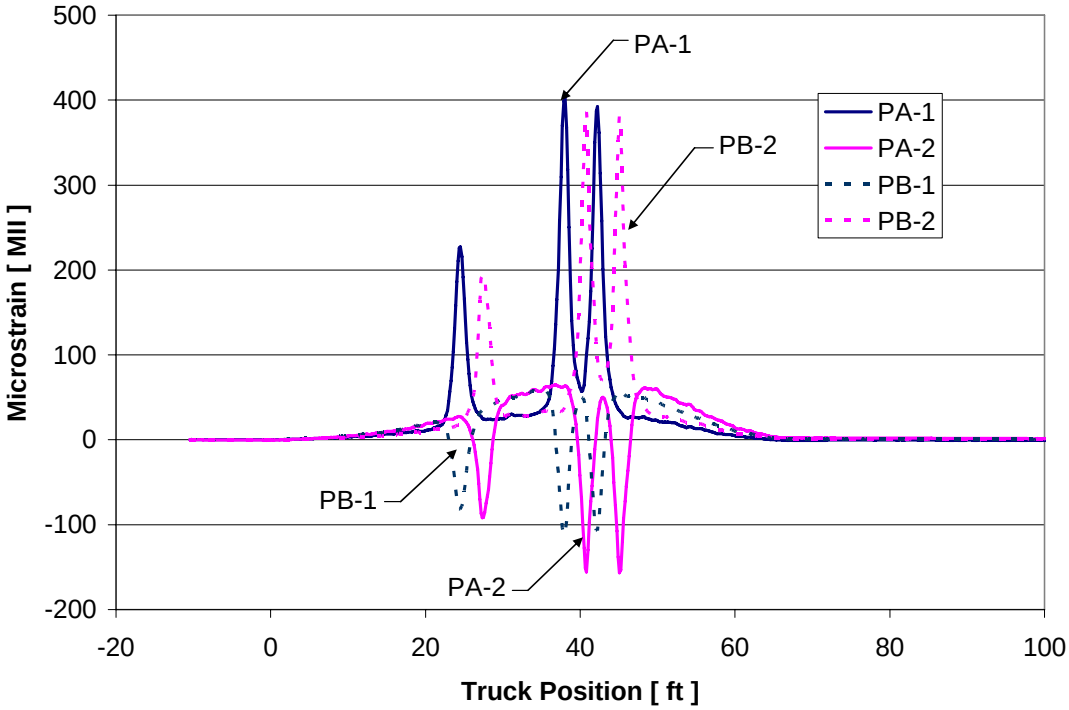

Figure 29. FRP Deck Strains: Path Y3 – 2003 Test

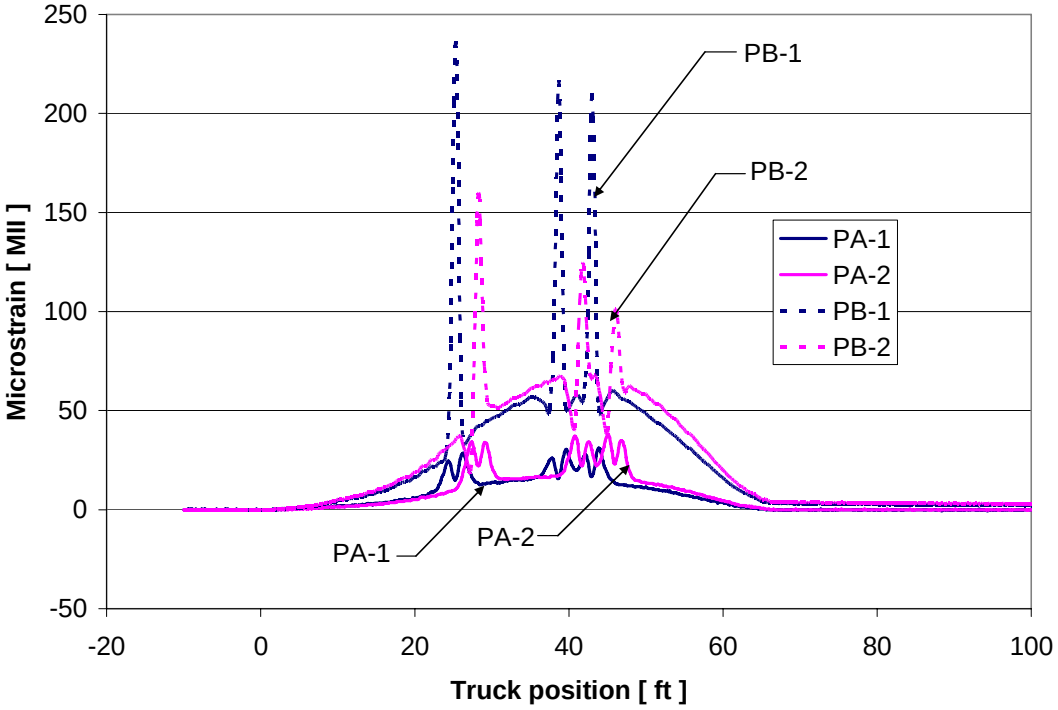

Figure 30. FRP Deck Strains: Path Y4 – 2004 Test

4.1.2. Strains Recorded on PC Girders

Recall that the PC girder strains were measured on the top and bottom flanges of the girders. The strain results from 2004 were multiplied by 1.024 to account for the difference in truck loading between the two tests. As expected, the most heavily loaded girders for Path Y1 were B, C and D. In the FRP-deck span, the changes over one year were less than 5% on the bottom flange, while on the top flange were up to 13% (Figure 31, Figure 32 and Figure 33). Similarly, the RC deck span girders had differences no larger than 7% on the bottom flange and 26% on the top flange.

It should be noted that the strain data in the FRP-deck span showed noticeable spikes in the top flange data as the truck wheels were in the area surrounding the sensors. This can be attributed to the lower stiffness of the FRP composite deck as compared to the concrete deck.

Along Path Y2, the wheel lines were closer to the Girders C and D and they were observed to be the most heavily loaded. Figure 34, Figure 35, Figure 36, and Figure 37 present the strain data for Girders B, C, D and E and allow comparisons for changes in strain magnitudes and general behavior over the time. For the FRP-deck span, the results showed that strain increments were up to 7% higher on the top flange and up to 1% higher on the bottom flange in 2004. The RC deck span showed increments up to 4% higher in the bottom flange and 5% higher in the top flange. Note that in Figure 37, the top flange of Girded E had strain readings in 2004 that were approximately 39% below than those in 2003. The cause of this change is not positively known. However, the fact that the top flange gages were placed on opposite sides of the girders coupled with torsional effects discussed later are believed to be a likely cause.

When comparing both spans, it is observed that the girder strains were larger in the FRP-deck span than in the RC-deck span. Typically, the bottom flange strains were 30% larger and the top flange strains were up to 500% higher. These comparisons were made without taking into consideration the span lengths, which could further increase that difference by a factor of approximately 1.3 for equivalent span lengths if the same girders were used (i.e., a total of 39% and 650% for the top and bottom strains respectively). As discussed in Chapter 3, and illustrated by the collected data, the FRP-deck span exhibited almost no continuity with the adjacent span, while the RC deck span appeared to be fully continuous with the adjacent span. This may have a significant influence on the moments induced in each span (i.e., this infers that the positive region moments of the FRP-deck span will not be reduced due to continuity as would the RC deck span in the positive region moments).

The higher strain levels in the FRP span are primarily attributed to the much lower stiffness of the composite FRP deck/girder section. To understand the behavior of the FRP-deck span, and how it relates to conventional design practice, the load distribution fractions, based on strain data, were computed. Also, the level of composite action, based on the neutral axis location, was computed and compared with theoretical calculations provided by The Schemmer Associates and the AASHTO Standard Specifications (1996). Additionally, when applicable, comparisons were made with the AASHTO LRFD Specifications (1998).

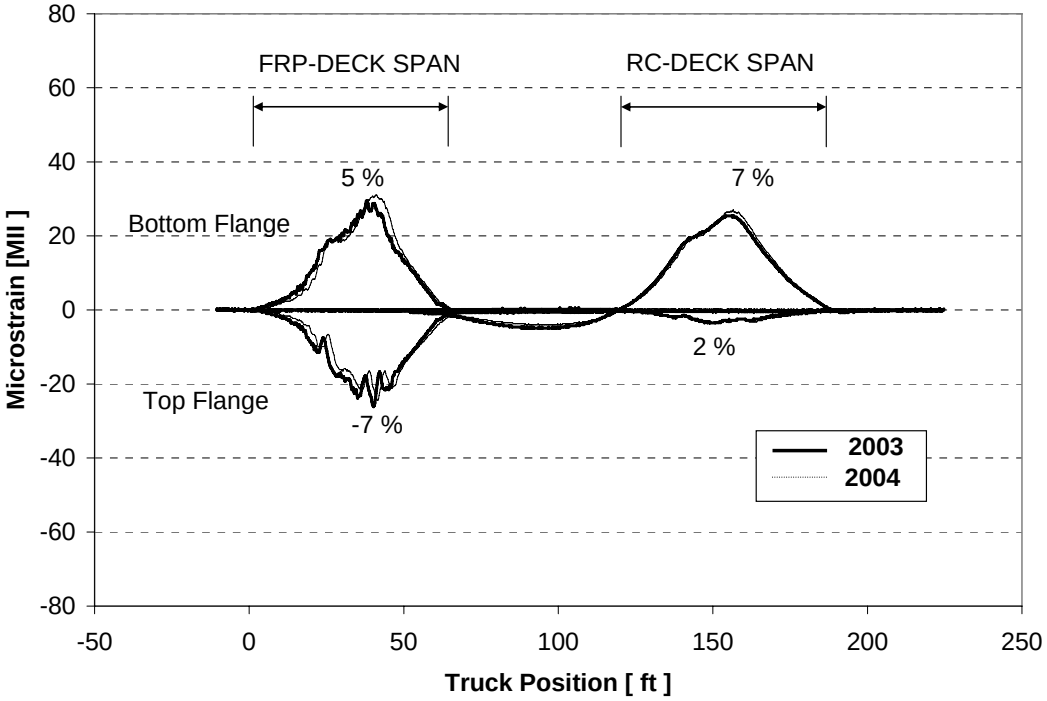

Figure 31. Strain Response Comparison: Girder B – Path Y1

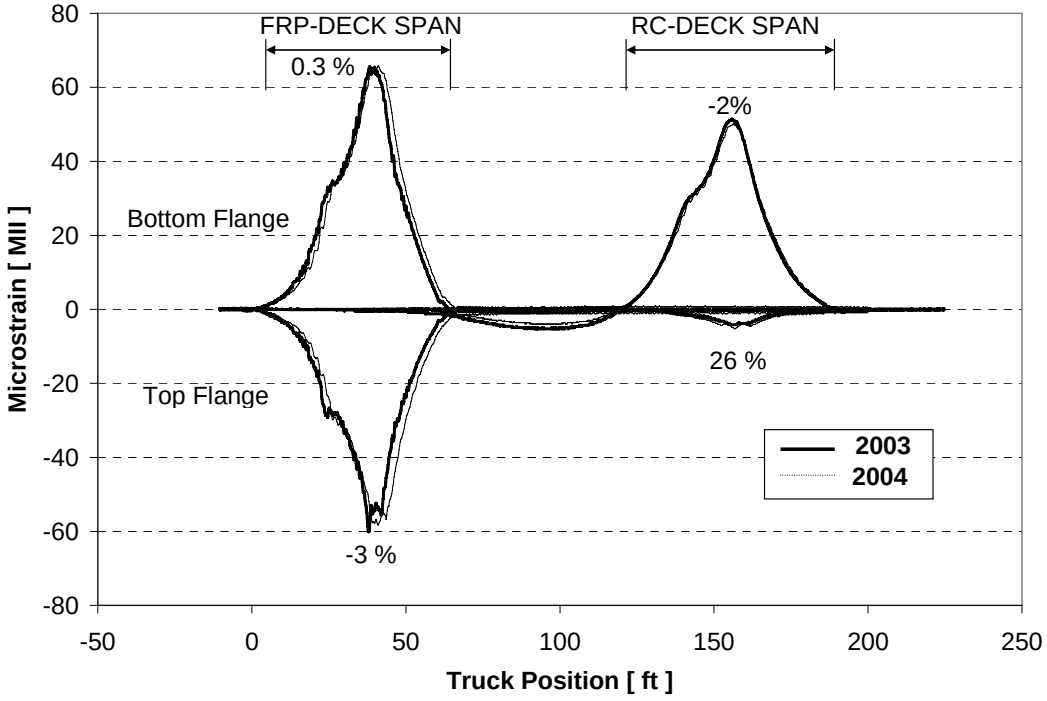

Figure 32. Strain Response Comparison: Girder C – Path Y1

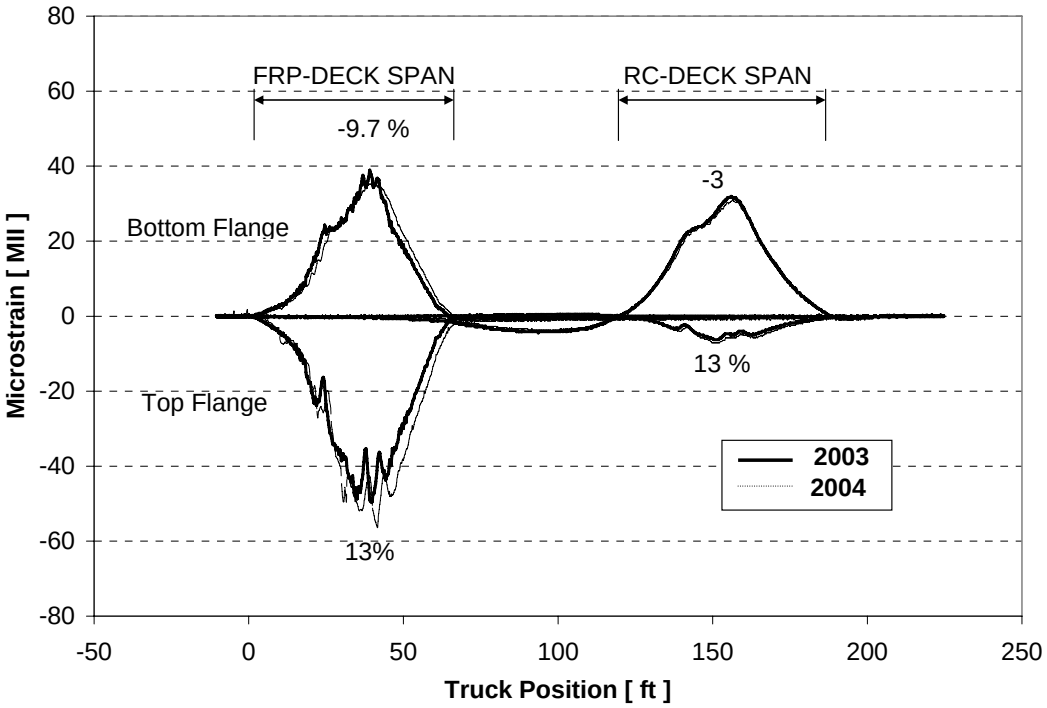

Figure 33. Strain Response Comparison: Girder D – Path Y1

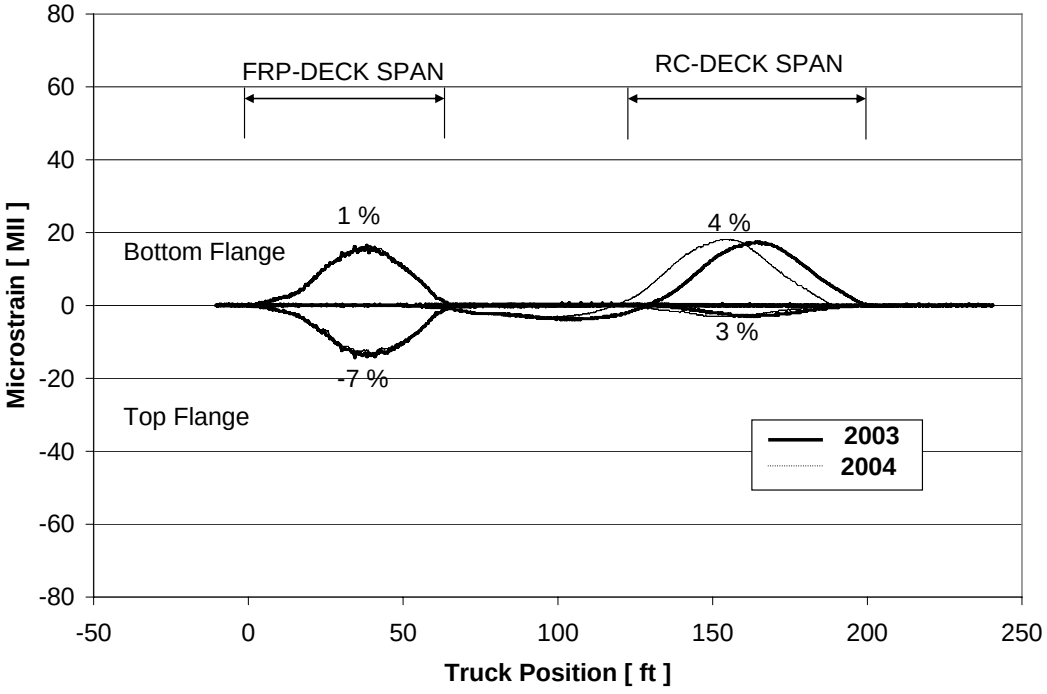

Figure 34. Strain Response Comparison: Girder B – Path Y2

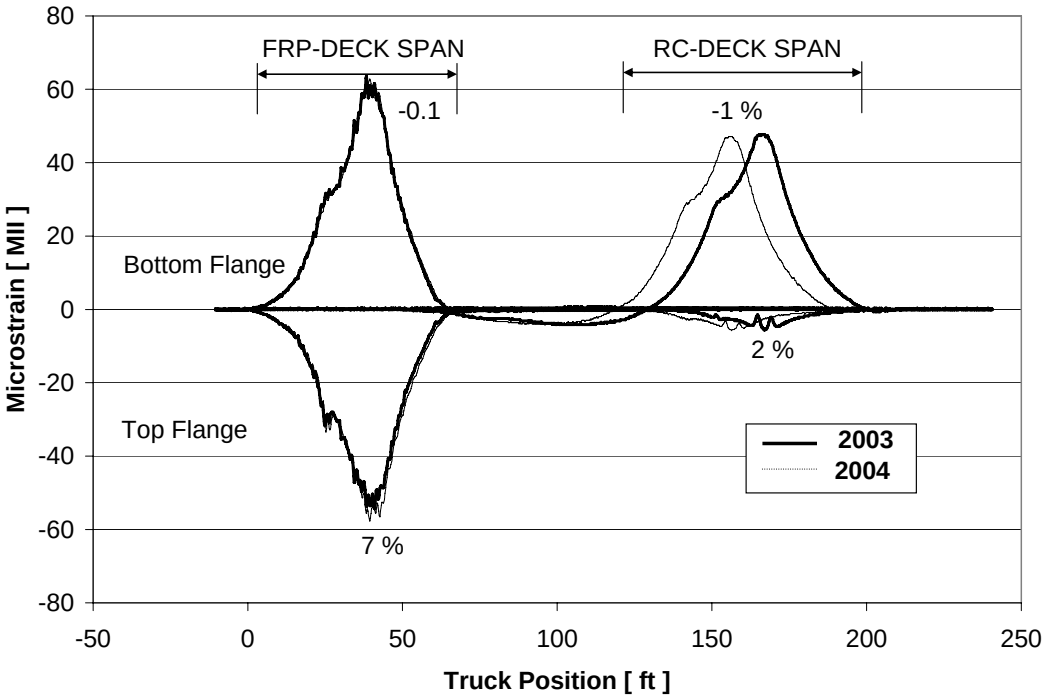

Figure 35. Strain Response Comparison: Girder C – Path Y2

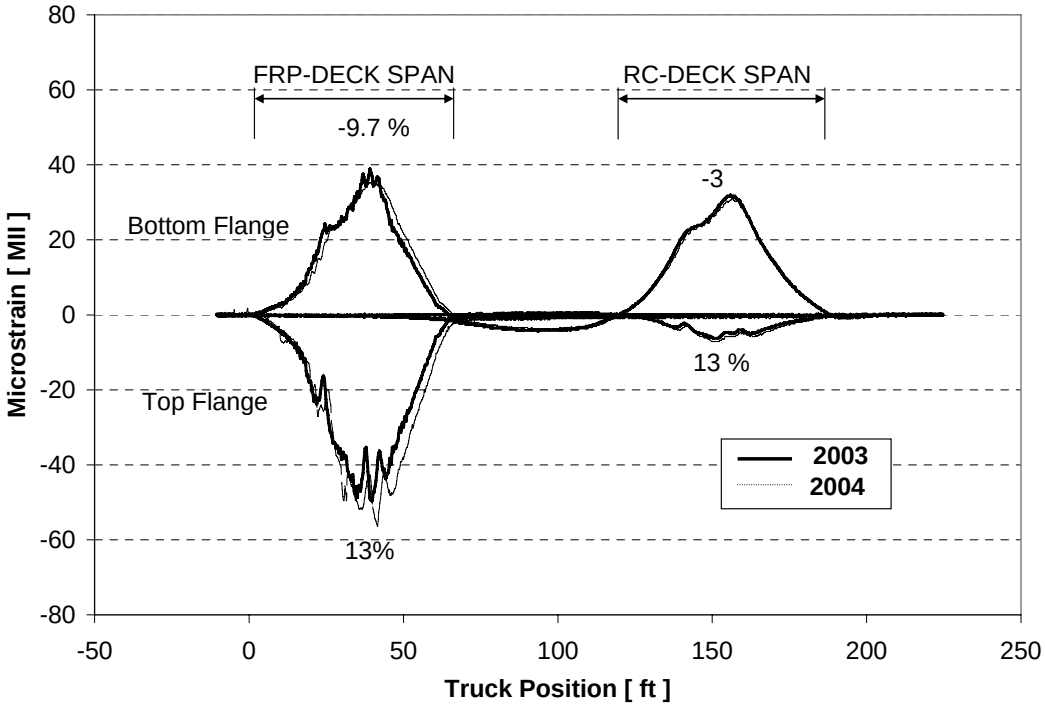

Figure 36. Strain Response Comparison: Girder D – Path Y2

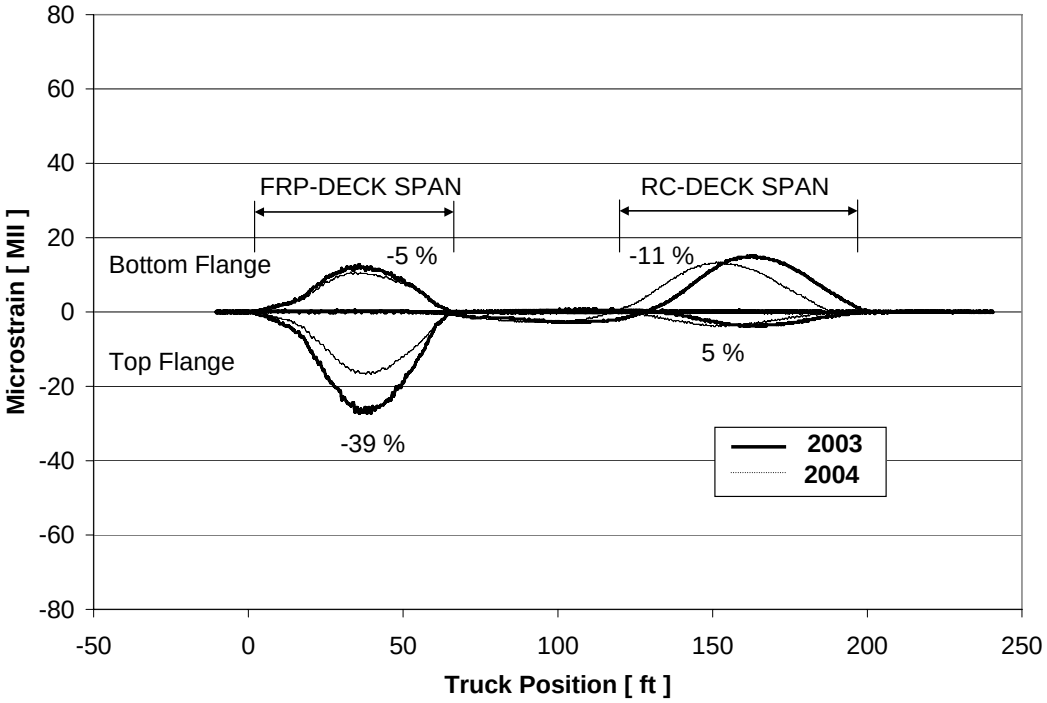

Figure 37. Strain Response Comparison: Girder E – Path Y2

4.1.2.1. Lateral Load Distribution

The effective lateral load distribution through the slab to the various girders was evaluated by determining an estimate of the LDF. The computation of the LDF from the field tests was based on the measured bottom flange girder strains. As expected, the most critical loading condition was Path Y1 (Figure 38). For the FRP-deck span, the LDF obtained was 47% in the 2003 Test and 43% in the 2004 Test, decreasing 8%. For the RC-deck span, the LDF was 43% for the 2003 Test, and 41% for the 2004 Test, decreasing 5%. The obtained data indicated that the RC-deck span was more effective in laterally distributing the loading than the FRP-deck span.

The Path Y2 LDF, shown in Figure 39, illustrates the same pattern between the two tests with only minimal differences. Although Path Y3 and Path Y4 were not coincident during the two-year study, it was observed that the LDFs for both were lower than 47% (Figure 40 and Figure 41).

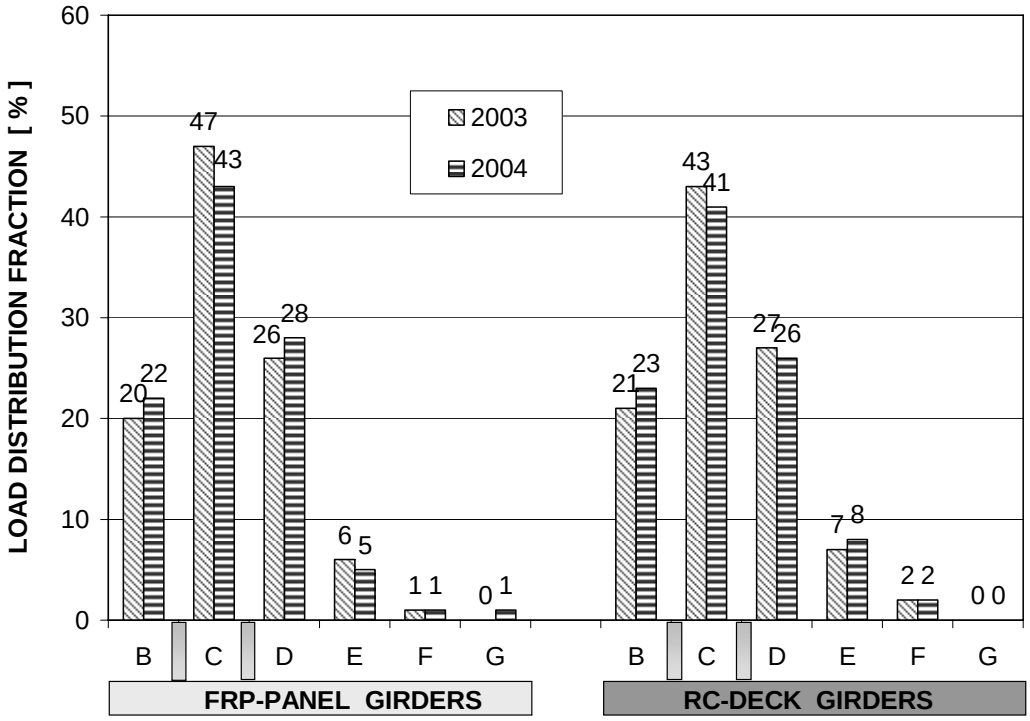

Figure 38. Path Y1 LDF

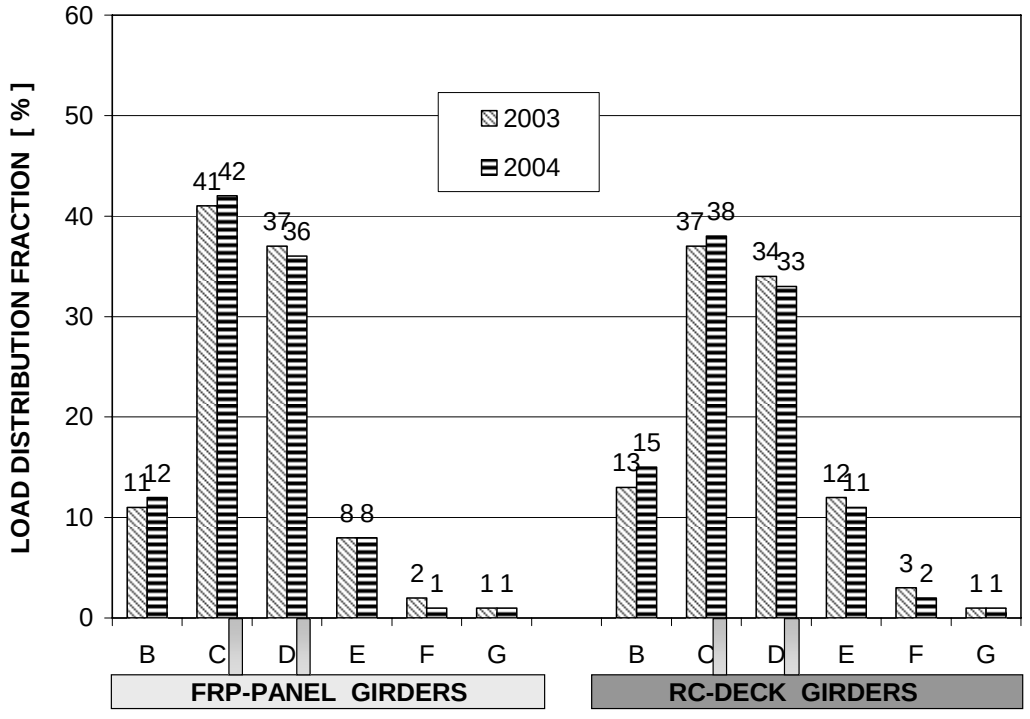

Figure 39. Path Y2 LDF

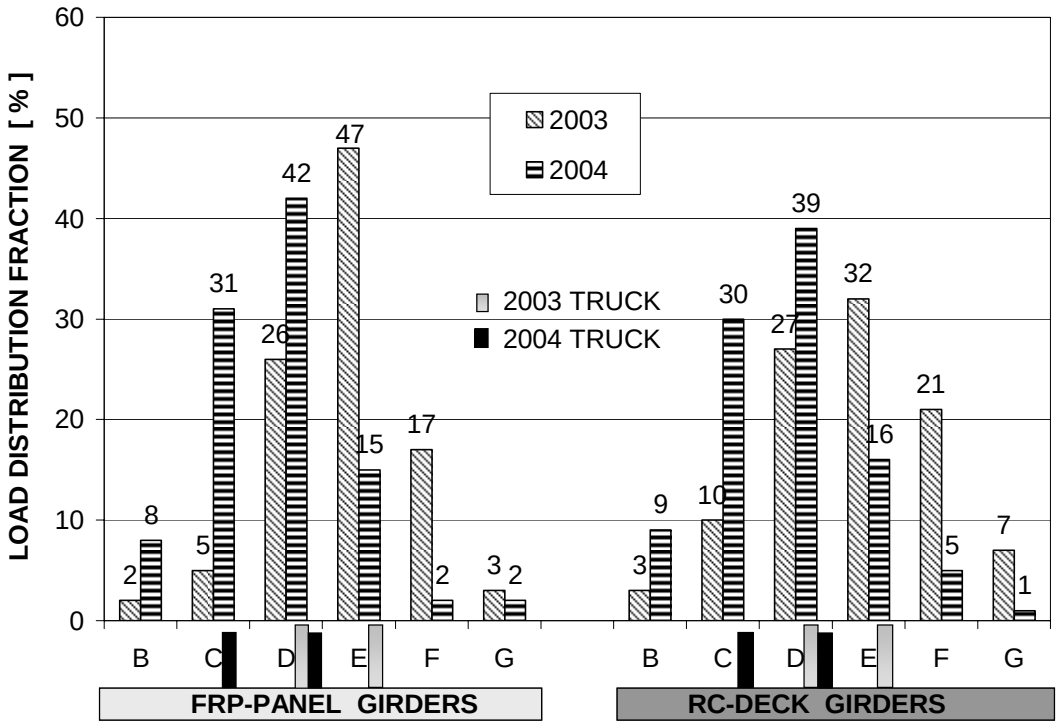

Figure 40. Path Y3 LDF

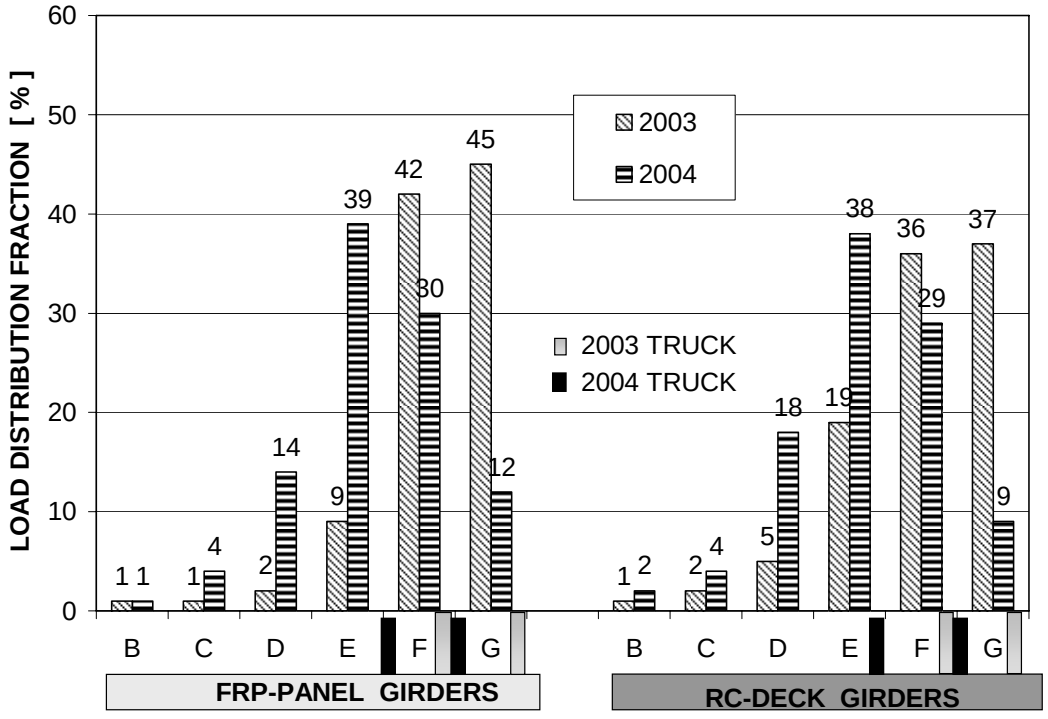

Figure 41. Path Y4 LDF

The LDF is defined as the fraction of the live load on each girder (AASHTO Standards, 1996). Since this bridge consists of five lanes, the design LDF was calculated as S/5.5 for two or more traffic lanes where S is the girder spacing in feet. The AASHTO Standard Specification provides distribution factors in terms of truck percentage. In the absence of code specifications for FRP panel decks, it was assumed by the designer that all decks behaved like an RC deck. Thus, for both spans and a girder spacing of 7 ft – 1 in., the LDF was 64.4% per wheel line (1.28 trucks). According to the AASHTO LRFD Specifications (1998), the LDFs are calculated based on the mechanical and materialistic properties of the composite section. Thus, the LDF was calculated to be 70.7% (1.41 trucks) for the FRP panel span and 62.7% (1.26 trucks) for the RC deck span. In the case of the FRP deck span, Figure 42 and Figure 43 show the LDF for three and two lanes, respectively computed by superimposing multiple passes of the test truck. The LDF per girder was calculated as a percentage of the superposition of bottom strains and assuming the linear elastic response of the bridge superstructure. As can be seen, the field results for Girders E and F were slightly lower than LFD and LRFD values. Figure 44 shows the LDF for the two tests over Path Y5 and Y6. Also, the test LDF were below the AASHTO values and no significant change was observed.

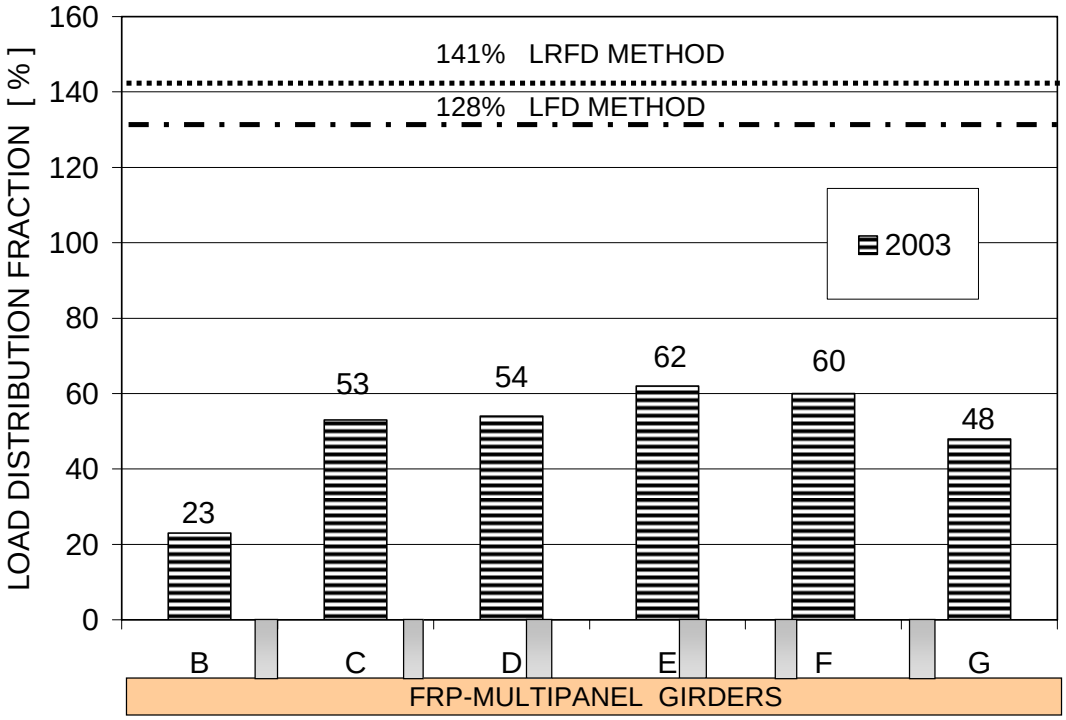

Figure 42. LDF Superposition of Paths Y1, Y3 and Y4

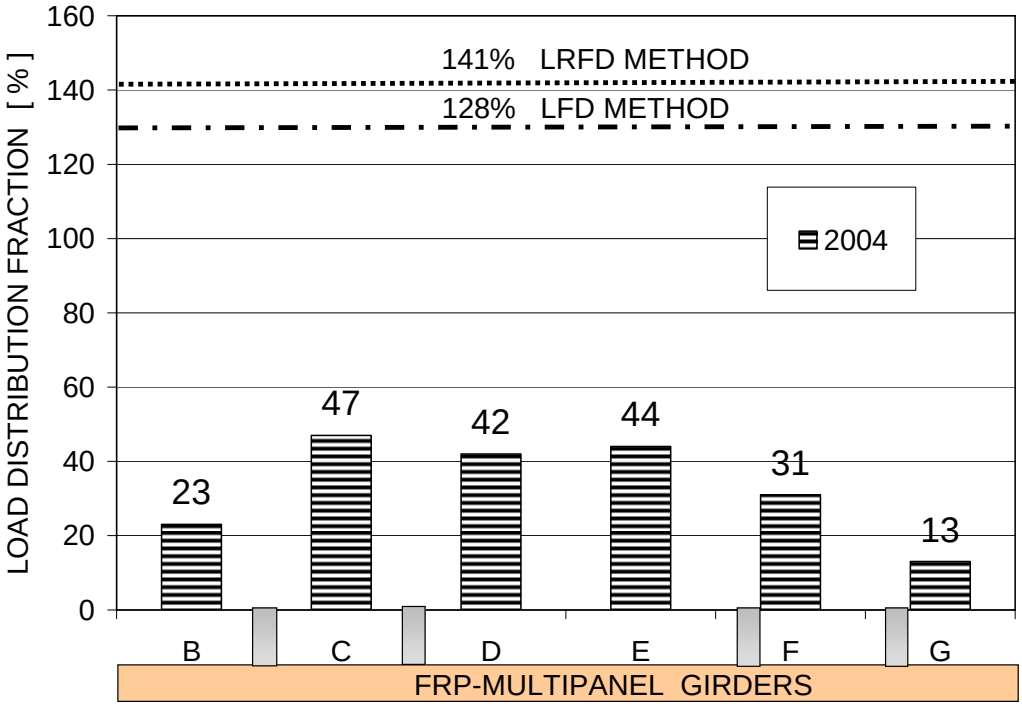

Figure 43. LDF Superposition of Paths Y1 and Y4

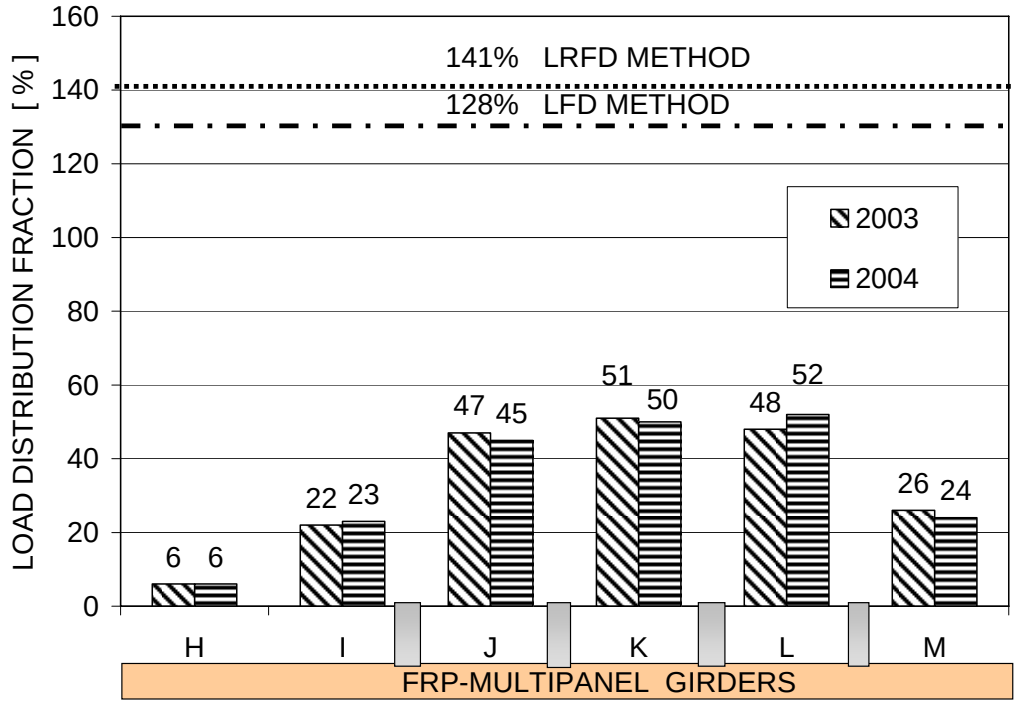

Figure 44. LDF Superposition of Paths Y5 and Y6

4.1.2.2. Neutral Axis Location

To evaluate the deck-girder interaction, the neutral axis of the composite section was computed based on the gage locations and strain readings obtained from the field test (Figure 45). As reference, the neutral axis location of the bare prestressed girder was calculated as 19.4 in. from the bottom flange, based on its geometry. Calculations provided by the designer of record, with assumed material properties, indicated that the neutral axis for each span, with full composite action, was calculated to be 23.5 in. and 38 in. from the bottom flange for the FRP-deck span and the RC deck span, respectively.

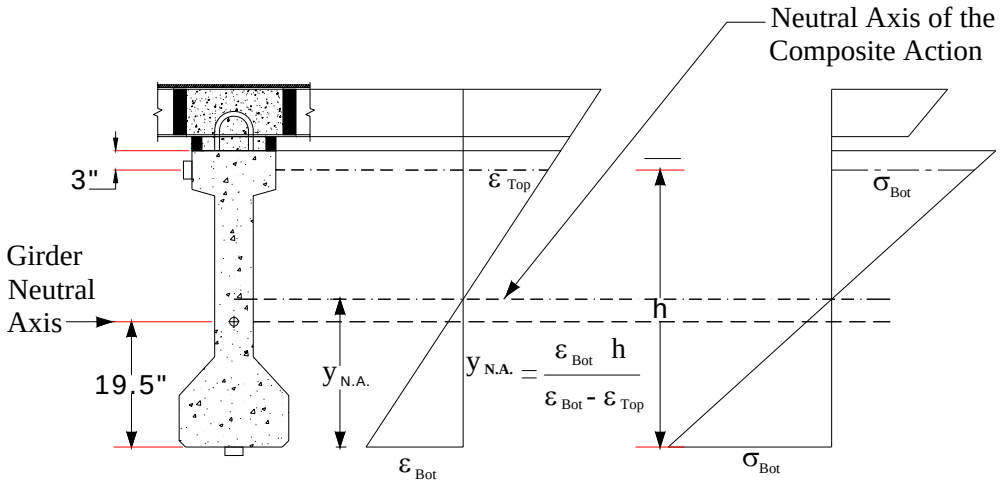

Figure 45. Evaluation of the Neutral Axis Location

The experimental neutral axis locations were determined for all transverse load positions. Figure 46 shows the neutral axis results for Path Y1 measured from the bottom flange over the most heavily loaded girders. As can be observed, the neutral axis locations did not significantly change over time. For Girders B and C, the values obtained show that composite action was likely achieved. For Girder D, the measured neutral axis location was below even the non-composite action (girder's neutral axis location, 19.4 in.). This can likely be attributed to a weak shear connection and the possibility of torsion effects of the truck loading typically ignored during design. This observation is validated later.

For Path Y2, Girders B, C and D were the most heavily loaded. Figure 47 shows the wheel positions relative to Girders C and D and the resulting neutral axis locations for both tests. Girder D's measurements again indicated a neutral axis position below the neutral axis of the girder alone.

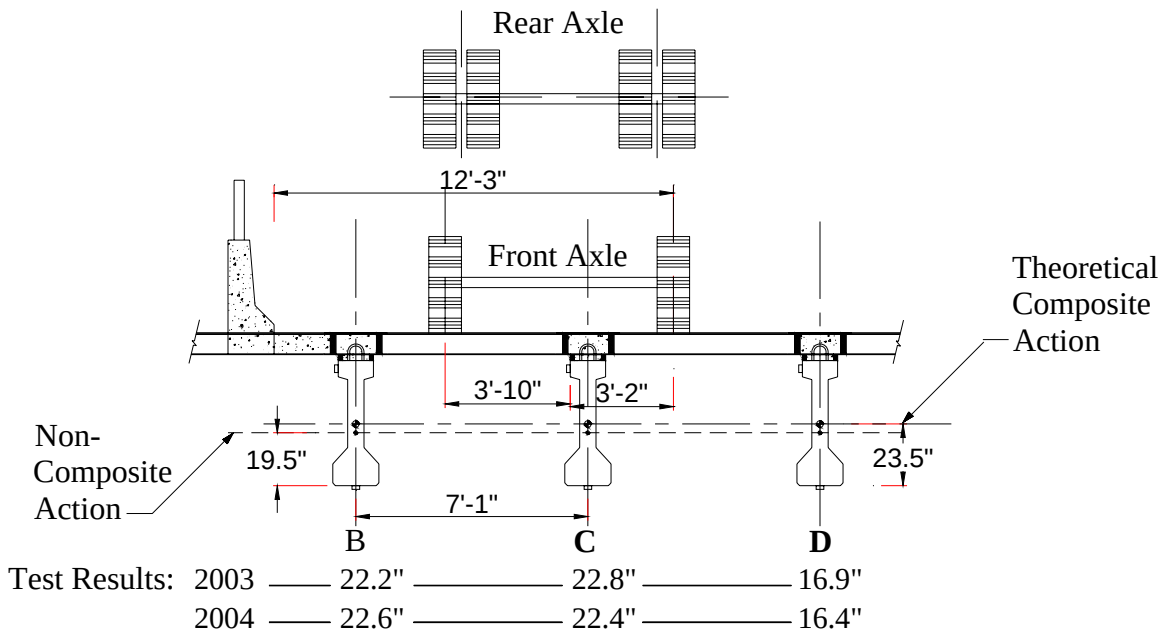

Figure 46. Neutral Axis: 2003 and 2004 Tests - FRP-deck span – Path Y1

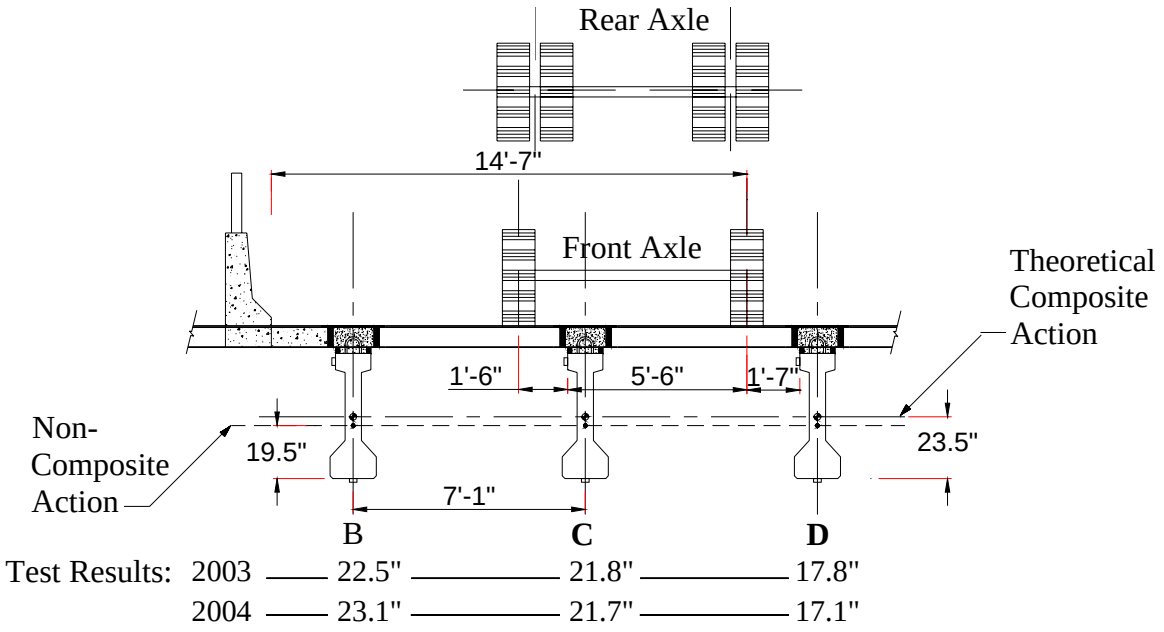

Figure 47. Neutral Axis: 2003 and 2004 Tests - FRP-deck span – Path Y2

Figure 48 shows the location of the neutral axis in the RC deck span for the two tests. The values were similar between the two tests and indicated that a high degree of composite action was likely achieved (design neutral axis of 38.0 in).

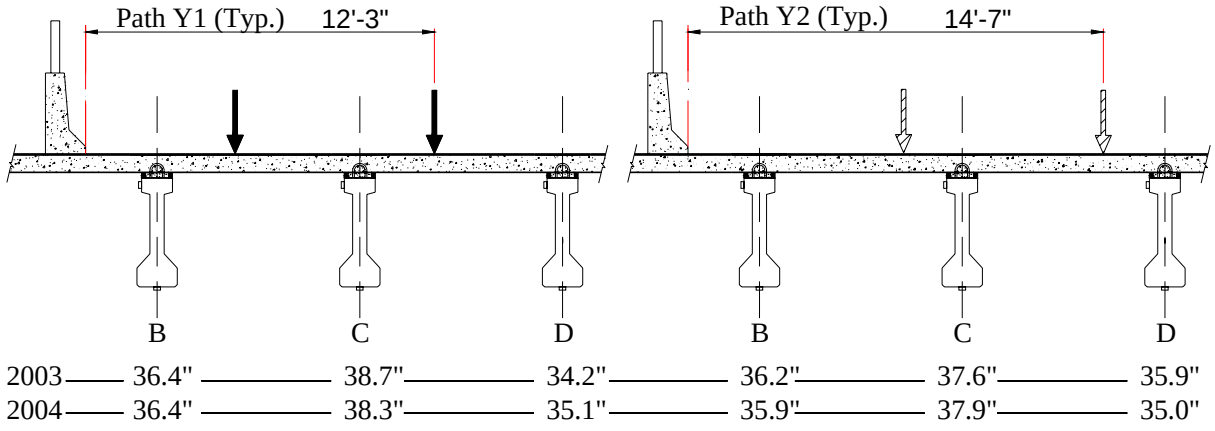

Figure 48. Neutral Axis: 2003 and 2004 Tests - RC Deck Span Comparison

To evaluate the impact of torsion in either Girder D or E, a single prestressed girder was modeled using a commercial finite element program. In this modeling, a three-dimensional element with simply supported ends and an intermediate diaphragm was used. The specific geometric and material properties used in the Bettendorf bridge were modeled. As shown in Figure 49, loads were placed at a position causing high live load beading stresses. Two specific cases were studied. In one case, the loading consisted of applying eccentric unit loads to cause torsion and bending in the girder. The other case considered centered loads applied on the girder which only caused bending.

The results of the torsional loading analysis showed that the absolute strains on the top flange were larger than the strains on the bottom flange, contrary to the results found for the flexural only loading analysis. It should be noted that for both loading cases, the same strain levels were obtained on the bottom flange. This can be explained as follows: without restraint (mid-span condition) the flange can warp and bend about the minor axis of the girder (Figure 50). Thus, the gage on the top flange captured two effects: pure bending and warping due to torsion. For the bottom flange, warping stresses are zero at the location when the strain transducers were placed. Thereby, when the neutral axis location was computed based on the gage positions and strains, similar to the field neutral axis computation, the increased top strain shifted the neutral axis down. For the torsional loading analysis, the obtained neutral axis was approximately 17 in., measured from the bottom flange, and was approximately 20 in. for the flexural loading analysis.

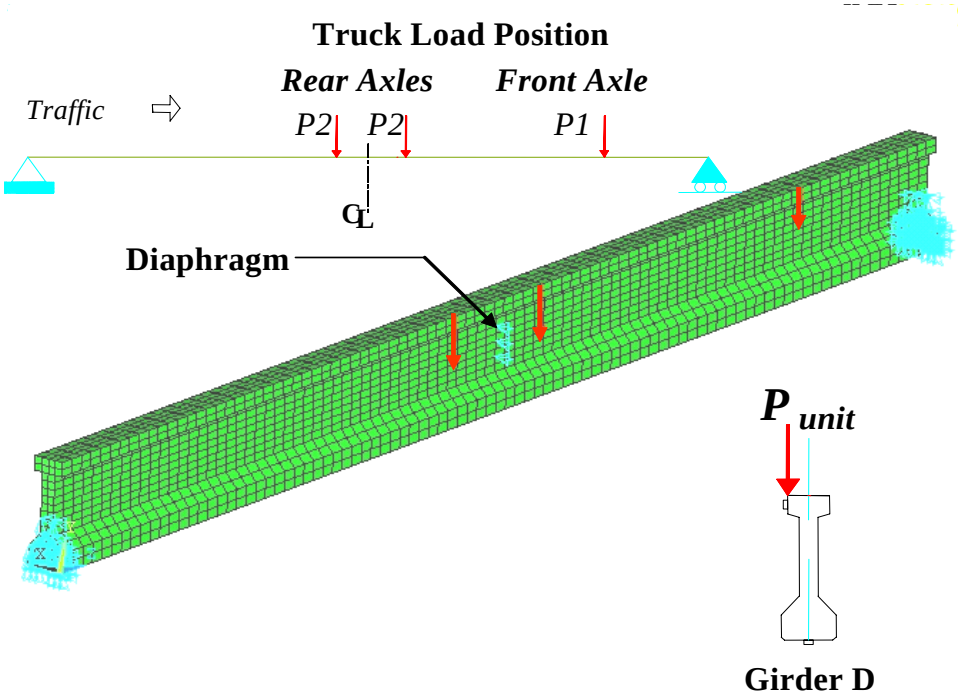

Figure 49. Analysis of Eccentric Load on Interior Girder D

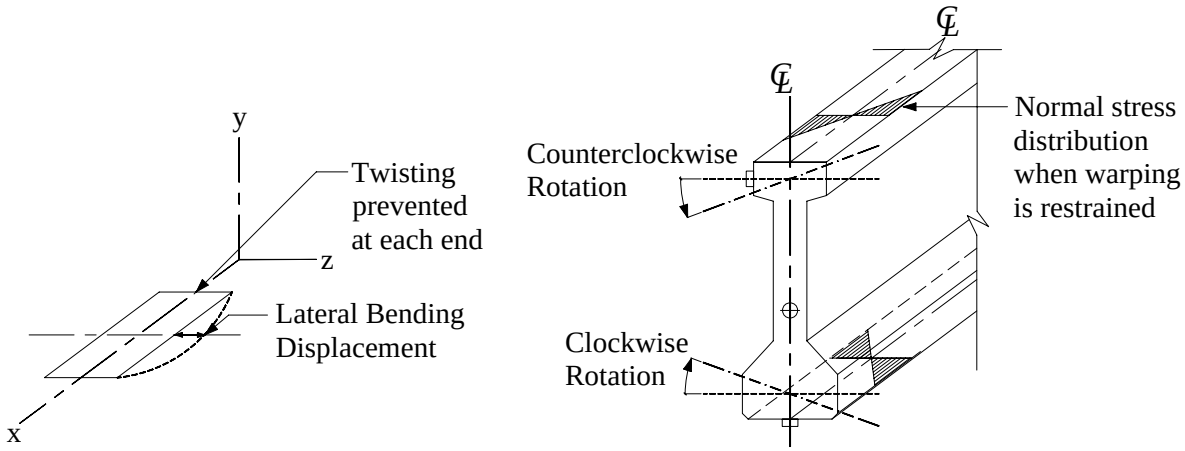

Figure 50. Effect of Warping Torsion

Finally, theoretical calculations, assuming full composite action, also revealed that the longitudinal composite RC deck-girder stiffness was approximately 3 times that of the composite FRP panel-girder. With this difference in longitudinal stiffness, along with the other factors previously mentioned (e.g., load distribution fraction, neutral axis location) but ignoring the continuity differences, from a girder design perspective, one could expect over 100% higher bottom flange live load stresses when using the FRP panel slab in place, in a “one-for-one”

replacement scenario, of a conventional concrete slab. It should also be noted that the top flange in-service load stresses would be, in statistical terms, much higher if the FRP panel slab was used in place of a conventional concrete slab (again in a "one-for-one" replacement scenario). However, it is likely that these stresses may not be critical as the increase is only large in statistical terms and not in absolute terms. It should also be pointed out that the FRP panel slab is much lighter than the conventional concrete slab. This would result in, for the same span length, lower dead load stresses in FRP panel slab span girders than in concrete slab span girders.

4.1.3. Deck-to-Girder Slip

Figure 51 shows the location of four slip-measurement transducers installed underneath the FRP panel on the top flange of Girders C, D and E. As expected, the differential horizontal displacement (slip) between the concrete girder and the FRP deck was found to be greatest when the truck was in the immediate vicinity of the instrumentation locations. The most critical case for these specific girders corresponded to Path Y2.

During the 2003 test, the peak measured slip, as shown in Figure 52, was 0.00226 in. and occurred when a truck tire was immediately over the instrumented section. Previous laboratory testing on the beam-to-slab connection (Wood et al, 2001) used in this bridge indicated that this level of slip (i.e., 0.00226 in.) corresponded to a horizontal shear force of approximately 9.8 kip or 26% of the connection's measured ultimate strength. It should be pointed out that the testing by Wood et al (2001) was completed on simple push out samples which can vary significantly from flexural members. Likewise, during the 2004 test, the maximum slip found was 0.004501 in. on Girder D North. The associated horizontal shear force was 19.5 kip, about 52% of the measured ultimate strength (Figure 53). Table 2 summarizes the differential deflections (i.e. slip) measured during the two-year tests for Girders C and D for Path Y2 which was the most critical case.

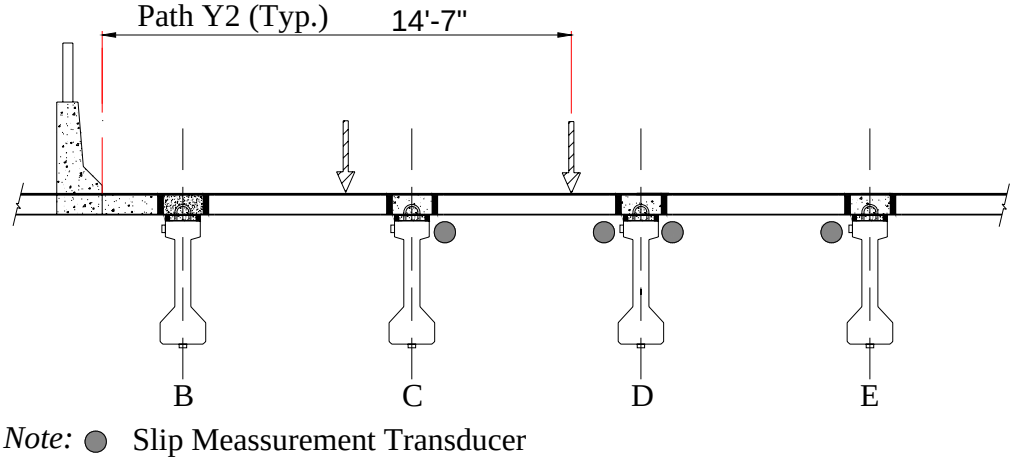

Figure 51. Location of Slip Instrumentation with Respect Path Y2

Table 2. Panel-to-Girder Slip: Path Y2

Position	*Year*	*Slip [in.]*
C South	2003	0.000371
	2004	0.000742
D North	2003	0.002265
	2004	0.004501
D South	2003	0.000512
	2004	0.000659
E North	2003	0.000282
	2004	0.000218

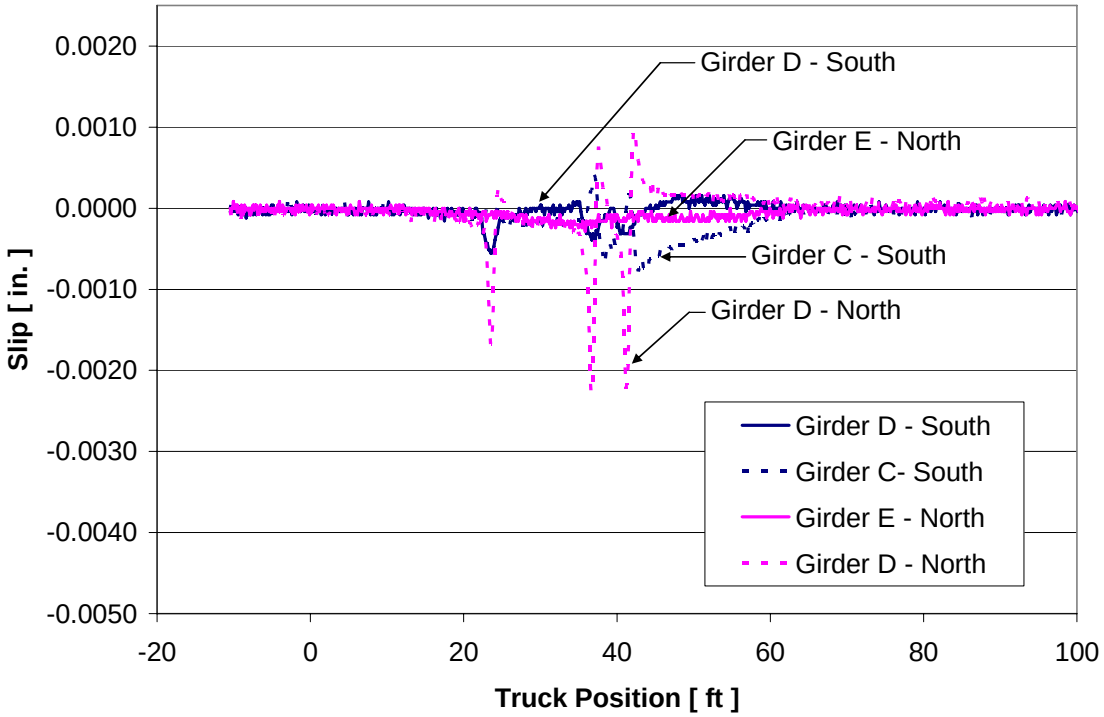

Figure 52. 2003 Path Y2 Deck-to-Girder Slip

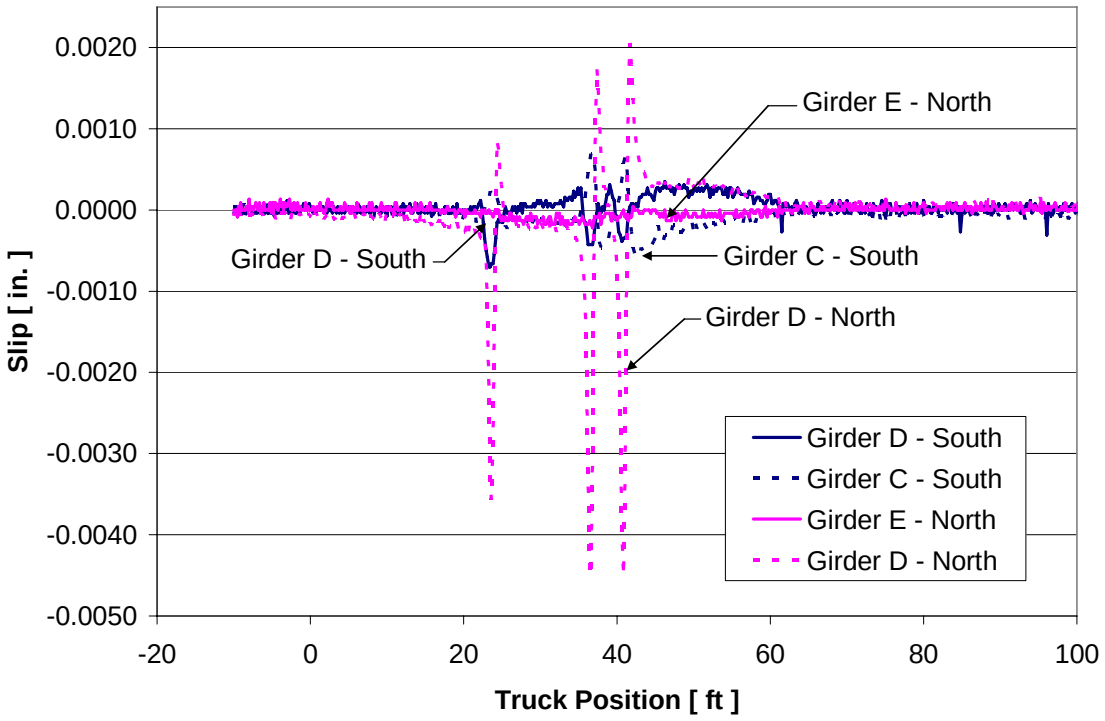

Figure 53. 2004 Path Y2 Deck-to-Girder Slip

4.1.4. Visual Inspection

During a walk-through inspection of the FRP deck in 2004, clear signs of cracking in the transverse direction of the traffic were found (see Figure 54 and Figure 55). Even though the joints cracked, the measured responses over time indicate that there was no significant loss of stiffness in the FRP deck. Thus, it is unclear what impact this cracking will have on the long-term bridge behavior.

Figure 54. Transverse Cracks in North Traffic

Figure 55. Transverse Cracks in South Traffic

4.2. Long-Term Monitoring Results

Figure 56, Figure 57 and Figure 58 illustrate three representative graphs of peak strain versus time. As can be seen in these graphs, the girders each reached peak strains that were between 650 and 750 MII. The consistency between the peak strains for the various girders indicates that there were very small differences in the response of the girders. It should be pointed out that 650

to 750 MII assuming an modulus of elasticity of 4 ksi corresponds to stress levels in the range of 2.6 to 3.0 ksi and are significantly higher than the strain levels measured during short-term testing. It was found, to the surprise of the research team, that the peak strain gages used in this work were not temperature corrected as the manufacturer had claimed. Therefore, the peak strain recorded by the sensors was the peak of temperature strains plus live load strains. In this case, the strains induced by temperature effects are several times greater than those one would expect under live load. Thus, the research team used a different approach to assess whether damage had occurred. To accomplish this, the research team analyzed the air temperature and active strain data (which when the bridge is unloaded represents temperature strain only) to identify changes in bridge stiffness. Although not a direct assessment of the likelihood of overload, when combined with the visual inspection results presented herein, the research team believes that the observed deterioration was the result of an overload event. Shown in Figure 59, Figure 60 and Figure 61 are examples of the temperature and active strain data for select girders. As can be seen, there is good correlation between the active strain levels and the ambient air temperature. This indicates that the girders were consistently responding to changes in temperature and that there was not likely any damage that would have occurred from an overloaded truck.

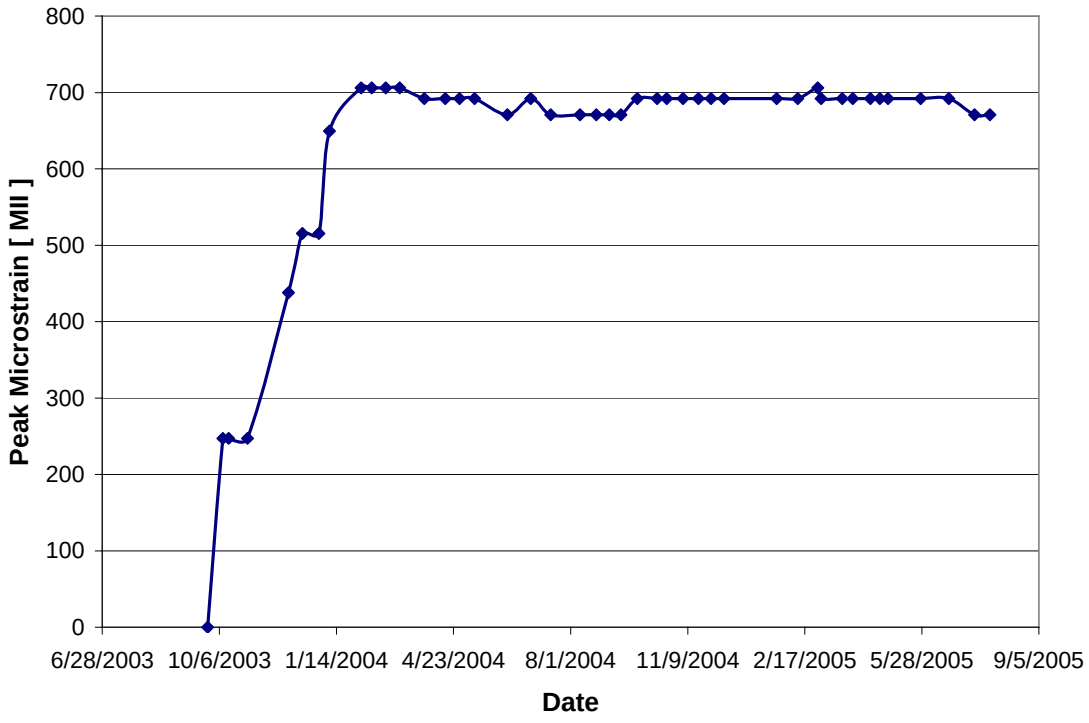

Figure 56. Girder B: Peak Strain Results

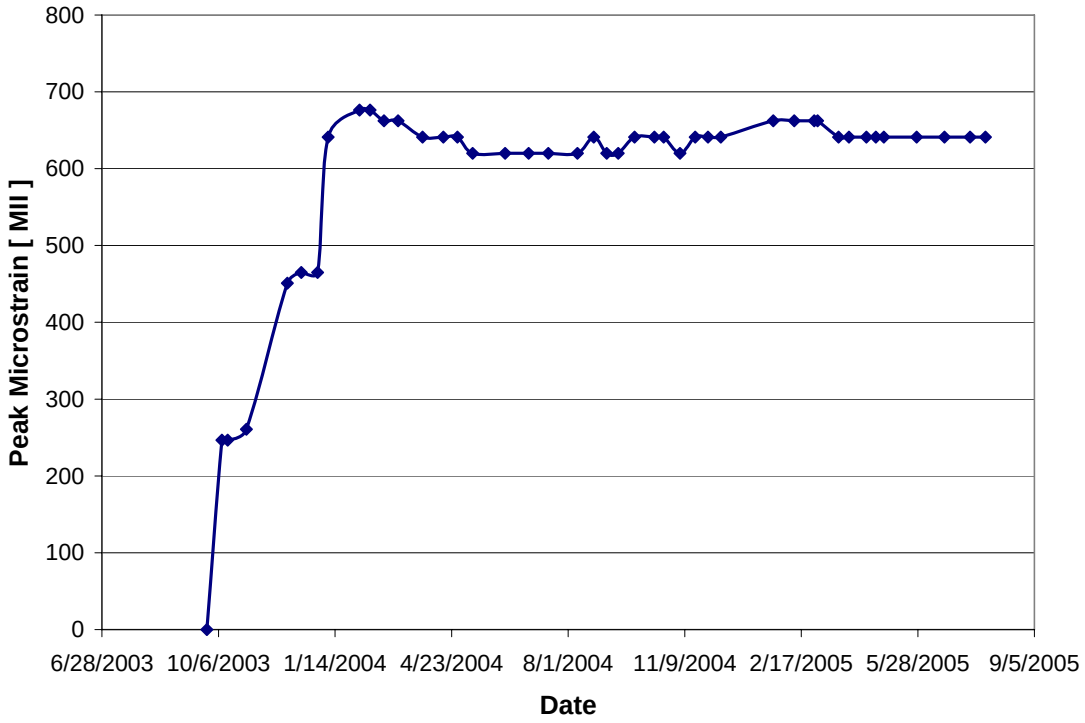

Figure 57. Girder E: Peak Strain Results

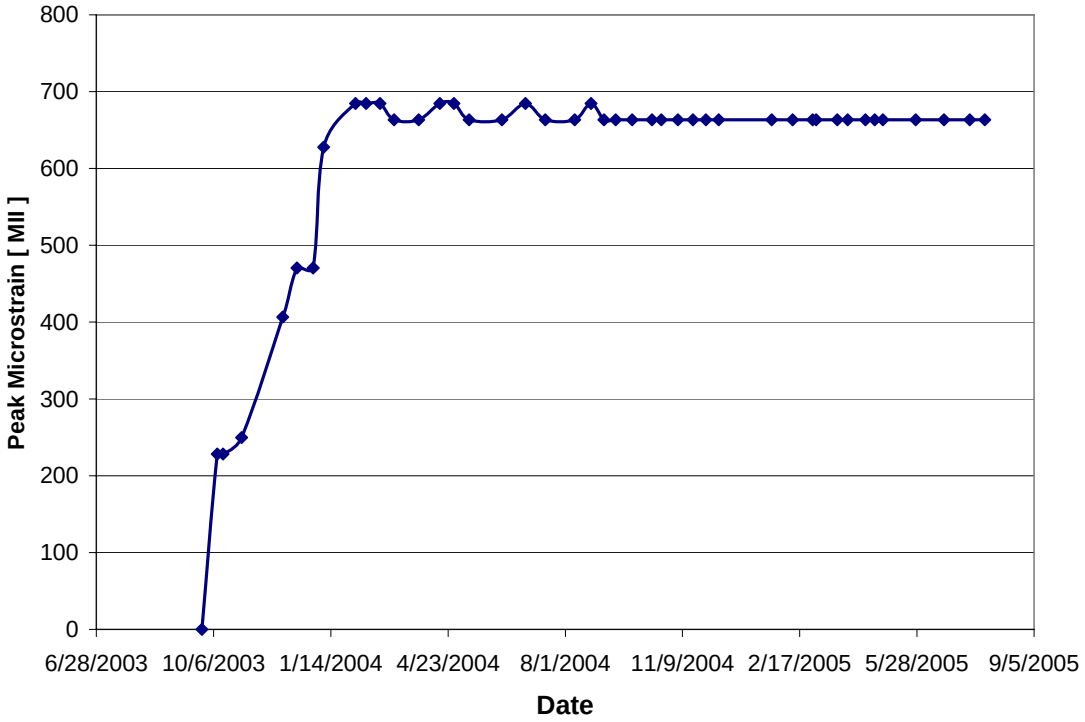

Figure 58. Girder L: Peak Strain Results

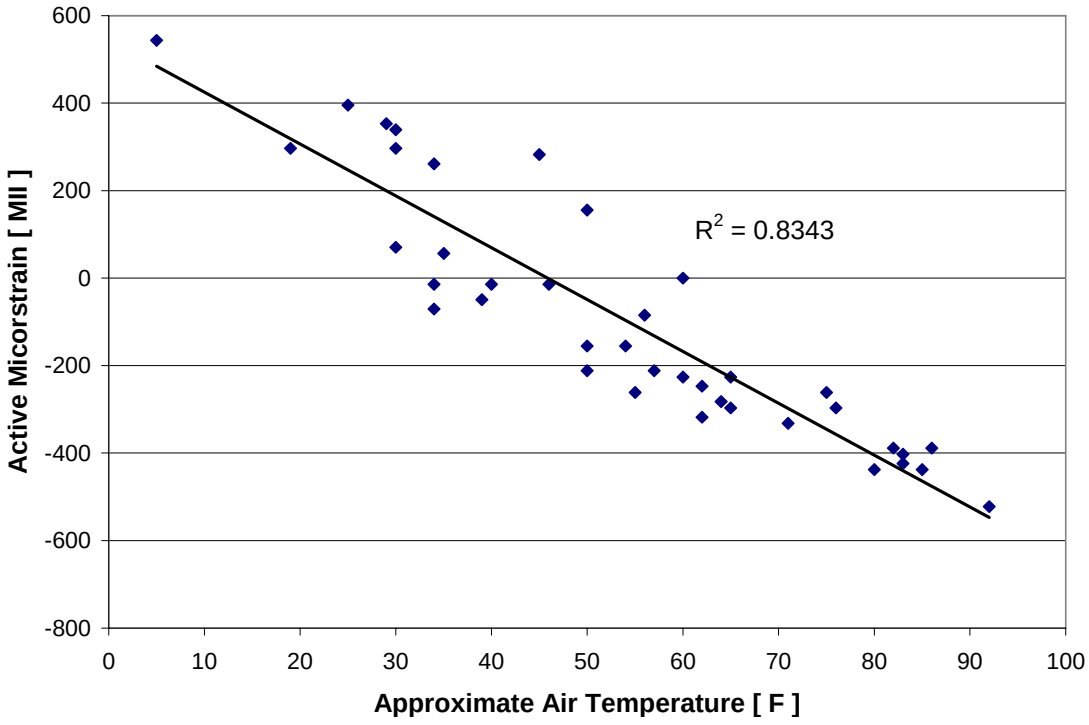

Figure 59. Girder B: Relationship Between Active Strain and Temperature

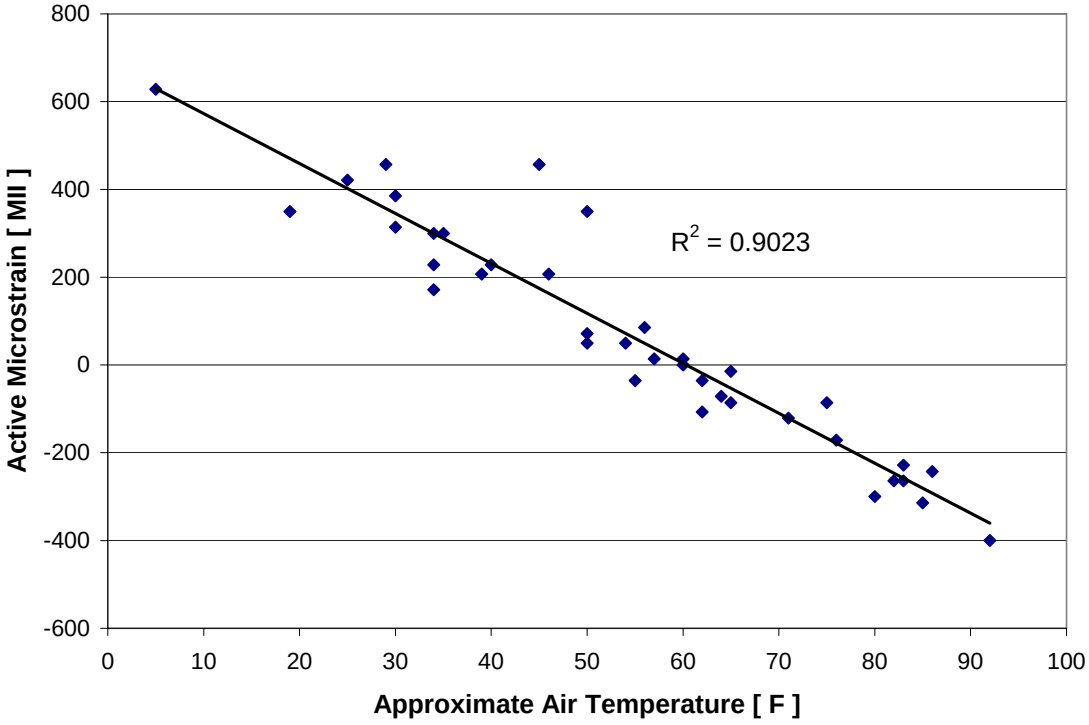

Figure 60. Girder J: Relationship Between Active Strain and Temperature

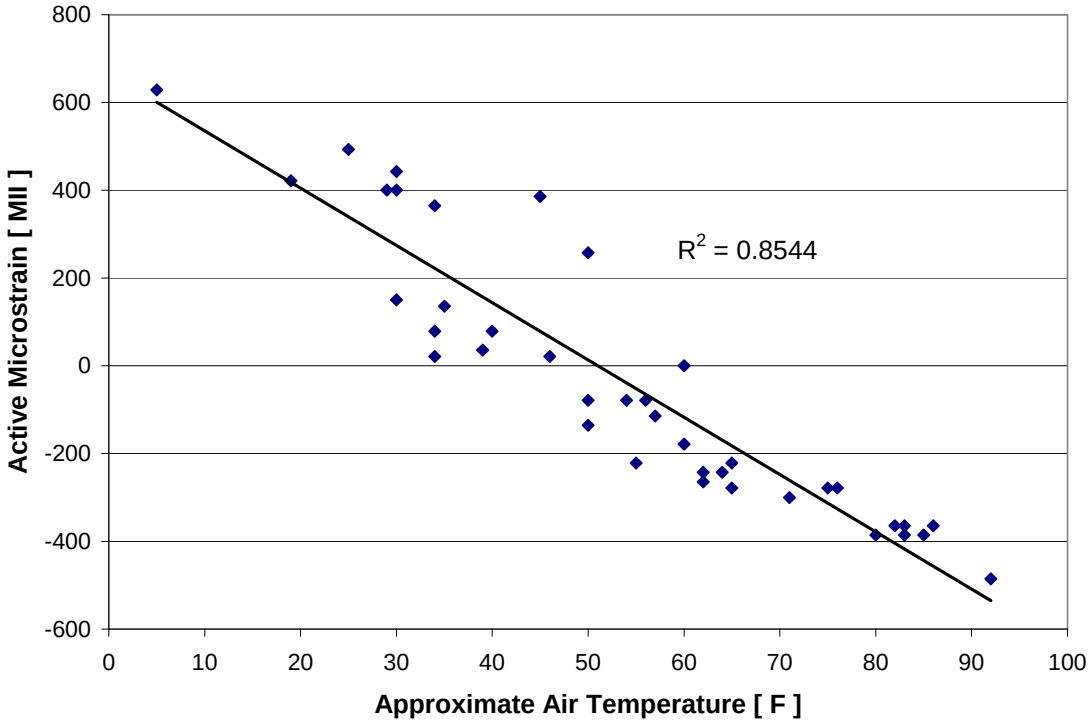

Figure 61. Girder M: Relationship Between Active Strain and Temperature

5. OBSERVATIONS AND CONCLUSIONS

The following field observations were made:

- After one year of service, clear signs of cracking in the transverse direction to the traffic were observed. Those cracks run parallel with the FRP tube components of the panels.
- No damage of the girders was observed.

The following conclusions are drawn from the short-term monitoring study:

- The FRP panels appear to be behaving elastically.
- From the PC girder strains, the strain readings indicate similar strain levels over the test period. Variations in strain over time indicate that there had been no decline in flexural stiffness.
- The load distribution fractions calculated from field test indicated no significant change from 2003 to 2004.
- The load distribution fractions computed for two and three lanes were lower than the AASHTO Standard and AASHTO LRFD Specification values.
- In general, it was observed that some intermediate girders may not have fully attained composite action with the FRP deck. Despite this, the strain levels measured were below the design strains.
- The deck-to-girder slip data indicate that there is a small relative displacement between deck and girders. These displacement magnitudes are still below the experimental results which provided the lower bound ultimate strength capacities for the shear connector detail.

The following conclusions are drawn from the long-term monitoring study:

- It does not appear that any unusually large loads crossed the bridge during the two year monitoring period. Thus, the observed deterioration is likely due to structural behavior effects and not loading effects.

6. REFERENCES

1. American Association of State Highway and Transportation Officials. (1996) "Standard Specifications for Highway Bridges Sixteenth Edition" Washington D.C. 20001.
2. American Association of State Highway and Transportation Officials. (1998) "AASHTO LFRD Bridge Design Specifications Customary U.S. Units Second Edition." Washington D.C. 20001.
3. Timoshenko, J. C. (1997) "Resistance of Materials" 3rd Edition, Prentice-Hall, Inc. Upper Saddle River, NJ, 939 pp.
4. O'Connor, J. (2004) "FRP Decks and Superstructures: Current Practice, Bridge Technology, U.S. Department of Transportation, Federal Highway Administration. Last time accessed: September 2005. http://www.fhwa.dot.gov/BRIDGE/frp/deckprac.htm.
5. Wood, D., Wipf, T.J., Klaiber, F.W. (2001) "Connection Tests of FRP Deck Specimens for Composite Construction." Iowa State University – Civil and Construction Engineering – Structural Engineering Laboratory, Ames, Iowa.
6. Birdge Diagnostic, Inc. (2002) "Load Test and Rating Report – Fairground Road Bridge, Greene County, Ohio", Boulder, Colorado. http://www.bridgetest.com/Greene.pdf
7. Keller, T. (2004) "Fiber-Reinforced Polymer Bridge Decks, Status Report and Future" Last time accessed: September 2005http://www.cobrae.org/afbeeldingen/paperkeller.pdf
8. GangaRao, H. (2004) "Thermal Response of Fiber Reinforced Polymer Composite Bridge Decks". CFC News, Constructed Facilities Center, West Virginia University, West Virginia.
9. Martin Marietta Co. (2005) "DuranSpan – Firber Reinforced Polymer Bridge Deck Systems. Thermal Response of Fiber Reinforced Polymer Composite Bridge Decks". Last time accessed: September 2005. http://www.martinmarietta.com/Products/DuraspanV1.pdf
10. Iowa Department of Transportation (IADOT). (2004) "Geographic Information Management System". GIMS_Roads 2004. Last time accessed: February, 2006.